CHARACTERIZATION OF *BOSEA* SP. WAO AND EXPLORATION OF CHEMOLITHOAUTOTROPHIC GROWTH ON LEAD AND ANTIMONY COMPOUNDS

by

ALEXANDRA B. WALCZAK

A dissertation submitted to

The Graduate School-New Brunswick

and

The Graduate School of Biomedical Sciences

Rutgers, the State University of New Jersey

In partial fulfillment of the requirements

For the degree of

Doctor of Philosophy

Graduate Program in Microbiology and Molecular Genetics

Written under the direction of

Lily Y Young

And approved by

_____

_____

_____

_____

New Brunswick, New Jersey

MAY, 2016

ABSTRACT OF THE DISSERTATION

Characterization of *Bosea* sp. WAO and Exploration of Chemolithoautotrophic Growth on Lead and Antimony Compounds

By ALEXANDRA B. WALCZAK

Dissertation Director:

Lily Y. Young

Microbe-mineral interactions are dominated by chemosynthetic microorganisms that use inorganic substrates for growth, impacting the formation and dissolution of minerals. In this dissertation, I continued to characterize *Bosea* sp. WAO using classical microbiological techniques and genomic analysis to better understand its physiology and ability to use inorganic electron donors for growth. This aerobic microorganism is capable of facultative chemolithoautotrophic growth on arsenite and several reduced sulfur compounds. It grows optimally at 25°C, pH 8, and is intolerant to salinity above 3.5 % w/v NaCl. Genomic analysis revealed that it contains the arsenite oxidase genes, *aioA* and *aioB*, and possesses the complete *sox* pathway. The draft genome is of a single circular 6,125,776 bp chromosome that contains 62 RNA genes and a predicted 5,665 protein-coding genes. A method for *in situ* stabilization of Pb

contamination is the addition of phosphate to convert redox sensitive sulfide minerals into sparingly soluble pyromorphite. I investigated the fate of reduced sulfur during the conversion of galena [PbS] to chloropyromorphite [$Pb_5(PO_4)_3Cl$] concluding with powder XRD analysis that the reaction results in the formation of elemental sulfur [S_8]. Under abiotic conditions the S_8 was retained in the solid phase, and negligible other sulfur species were detected in the aqueous phase. When PbS reacted in the presence *Bosea* sp. WAO the S_8 in the secondary mineral was oxidized to sulfate and significantly more sulfate was produced from the secondary mineral than from the primary PbS. Microscopic analysis of mineral particles indicated the organism was co-localized and grew on the secondary mineral surface. The results indicate that stimulation of sulfur-oxidizing activity may be a direct consequence of phosphate amendments to Pb contaminated soils. Four microorganisms, *Bosea* sp. WAO, *Starkeya novella*, *Thiomicrospira crunogena* EPR75 and *Halothiobacillus hydrothermailis* EPR 155, unable to utilize sodium tartrate as a carbon source, were used to study chemolithoautotrophic growth on antimony, Sb(0) and Sb(III). These organisms did not grow on either elemental antimony or potassium antimony tartrate. *Bosea* sp. WAO's initial rate of sulfate production from the mineral stibnite (Sb_2S_3) was higher than the controls, suggesting the organism increases oxidation of the mineral.

Acknowledgements

I would like to thank the members of my dissertation committee: Dr. Lily Y. Young, Dr. Nathan Yee, Dr. Costantino Vetriani, and Dr. Tamar Barkay for their assistance in completing this dissertation work. I am thankful to my advisor Dr. Lily Y. Young and co-advisor Nathan Yee for their guidance, support, and encouragement. I want to thank Dr. Costantino Vetriani for his invaluable comments about sulfur oxidizing organisms and providing me with two of the microorganisms for the antimony project. I want to thank Dr. Tamar Barkay for her insights and feedback during group meetings and on this dissertation. I am indebted to Dr. Will Paxton who helped me find the lost sulfur. He noticed a tiny peak in my XRD data that allowed me to pull together the PbS story. I want to thank Dr. Gregory Druschel and his graduate student Fotios-Christos A. Kafantaris for invaluable help with sulfur speciation chemistry and for allowing me to visit their lab to conduct experiments. They have helped make significant contributions to chapter 3. I want to thank Noriko Kane-Goldsmith for her excellent confocal skills and willingness to successfully try imaging non fluorescent minerals. I greatly appreciate Dr. Elizabeth McCandlish for her assistance with all the ICP-MS analysis for antimony concentrations.

I want to thank all the members, past and present, of the Young lab who helped hash out experimental ideas and instrument challenges. A special mention to Maria Rivera for her tireless efforts to keep the lab running smoothly, Dr. Adam Mumford who assisted with genomic analysis and arsenic work, Sarah

Wolfson for the best brownies ever, Dr. Abigail Porter for discussions about student learning, and Dr. Jennifer Kist for being willing to proof read manuscripts.

A special thank you to Tiffany Louie for helping to edit this dissertation and many other grants, proposals, and applications. I want to thank the Yee, Reinfelder, and Barkay labs for all their insights at lab meetings and willingness to share supplies and instrumentation. I want to especially thank Dr. Madhavi Shah (Parik) for her assistance running the initial powder XRD samples and with preparing the genomic DNA for sequencing. I want to thank the many undergraduate students who helped with pieces of all my projects, Tracy Scott, Nilar Win, David Ozga, Kyle Oschell, and Amanda Adubato. Their assistance let me develop my skills as a mentor while having an extra set of hands to complete some of the more tedious aspects of projects.

Finally, I want to thank my funding sources: The New Jersey Water Resources Research Institute which funded much of the work presented here, especially the genome analysis and the Rutgers Aresty Undergraduate Research Center which funded several of the undergraduate students and their projects that directly related to my research.

Dedication

I dedicate this dissertation to my parents

Maria Borga and Timothy Walczak

For raising me to be persistent in the face of any challenge

Table of Contents

Pages

List of Tables

Pages

List of Figures

Page

Chapter 1:

Introduction and Literature Review

Geomicrobiology. The study of geomicrobiology encompasses the interactions between microorganisms and geological processes. Microorganisms through their metabolic activities are involved in both the formation (biomineralization) and dissolution (bioweathering) of minerals and play a significant role in shaping the biosphere (Ehrlich 1996, Gadd 2010, Konhauser 2007). These activities can affect metal speciation, toxicity and mobility (Gadd 2010). As shown in Figure 1.1 some biogeochemical processes mediated by microbes include: organic matter decomposition and cycling, changes in redox chemistry, altered distribution of elements, leaching and solubilization of metals and other soil components, and the stabilization and alteration of soil structure (Gadd 2010). Microbes alter the environment around them both by their metabolism and their physical growth due to their abilities to be filamentous, produce extracellular polysaccharides, sorb particles or act as nucleation points for minerals altering the surrounding soils, rocks, or plants (Gadd 2010). Microbes are necessary for geochemical cycling with their unmatched metabolic diversity allowing them to inhabit any niche that at least occasionally has water (Konhauser 2007).

I focus here on microorganisms that grow using chemosynthesis, producing energy from the oxidation of reduced inorganic compounds coupled with the reduction of oxygen and fixation of carbon dioxide. I will look at several

sulfur compounds, arsenic, and antimony, both metalloids from group 15, as electron donors for this process.

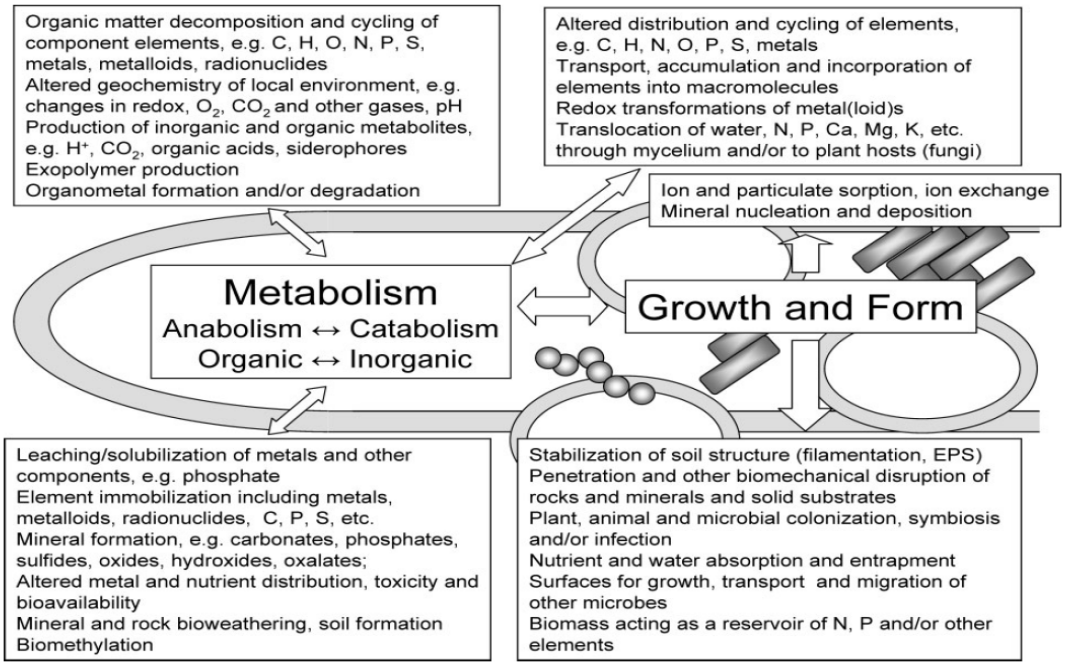

Figure 1.1. Important microbial activities related to the biogeochemical cycling of metals and the processes that change their distributions and speciation. These activities take place both in terrestrial and ecosystems and are frequently interlinked to mode of growth such as unicellular or filamentous and mode of metabolism which will depend on the nutrient and energy source availability (reproduced with permission from Gadd 2010).

Carbon Fixation. There are six known carbon fixation pathways: 1) the Calvin-Benson-Bassham Cycle, 2) the reductive acetyl-CoA pathway, 3) the reductive tricarboxylic acid cycle (TCA), 4) the 3-hydroxypropionate/malyl-CoA cycle, 5) the 3-hydroxypropionate/4-hydroxybutyrate cycle, and 6) the dicarboxylate/4-hydroxybutyrate cycle (Atomi *et al.*, 2002, Saini *et al.*, 2010, Berg 2011). In free-living aerobic chemosynthetic organisms, however, CO_2 fixation predominately occurs by the Calvin-Benson-Bassham Cycle (Shively *et al.*, 1998, Shively *et al.*, 2001 Berg 2011). Organisms can be obligate

chemoautotrophs and grow on a select number of reduced inorganic substrates or facultative chemoautotrophs and able to grow on a wide range of inorganic reduced substrates in addition to using organic compounds (Shively *et al.*, 1998). Chemoautotrophic growth can occur with the electron donors molecular hydrogen or reduced nitrogen, sulfur, metals, or carbon (Shively *et al.*, 1998).

The Calvin Cycle consists of 13 enzymatic reactions with the enzyme ribulose-1,5 bisphosphate carboxylase/oxygenase (RuBisCO) responsible for the carbon fixation step (Shively *et al.*, 1998). The cycle requires three molecules of CO_2 to form one molecule of triose phosphate using nine molecules of ATP and six molecules of NADH (Shively *et al.*, 1998, Berg 2011). RuBisCO is the most abundant protein in the world mostly due to its low catalytic efficiency and wasteful side reactions with oxygen (Berg 2011). There are four Forms (I, II, III, and IV) of RuBisCO with Form I and II participating in autotrophic CO_2 assimilation, while Form III belongs to the *Archaea* and is not been shown to be used for autotrophy (Atomi 2002, Berg 2011). Form I is found in all plants, algae, cycanbacteria, and most chemoautotrophs, while Form II is less common (Atomi 2002). Some bacteria have been shown to have both Form I and II such as *Rhodobacter*, *Thiobacillus*, and *Hydrogenovibrio* (Atomi 2002). The Form I enzyme is encoded by the *cbbL* and *cbbS* genes on the cbb_I operon while Form II is encoded by the *cbbM* gene in the cbb_{II} operon (Atomi 2002). It has been shown that bacteria containing different forms express them based on CO_2 availability with Form II for high CO_2 levels and Form I for low CO_2 levels (Berg

2011). The presence of these genes can act as biomarkers for RuBisCO and the Calvin-Benson-Bassham Cycle.

Sulfur Cycle and Microbial Activity. In the environment, sulfur cycles between being fully oxidized as sulfate and fully reduced as sulfide. Many of the intermediate redox reactions are both biologically and abiotically mediated. Sulfate can be reduced to organic sulfur compounds through assimilatory sulfate reduction or directly to sulfide through dissimilatory sulfate reduction by sulfate reducing bacteria (SRB) (Fig. 1.2) (Robertson and Kuenen 2006). This process is typically carried out by anaerobic bacteria that utilize the sulfate as their electron acceptor for metabolic processes (Friedrich 2001, Robertson and Kuenen 2006). In the other half of the cycle, reduced sulfur compounds (sulfide, elemental sulfur, polysulfides) can be oxidized to sulfur or sulfate by abitoic processes or biological oxidation that is either aerobic or anaerobic (Fig. 1.2) (Robertson and Kuenen 2006). Biological oxidation is mediated by sulfur oxidizing bacteria (SOB) that can either oxidize sulfide directly to sulfate or to sulfur as an intermediate (Robertson and Kuenen 2006). The microorganisms involved in the oxidation processes are always competing with naturally occurring abiotic reactions to obtain energy.

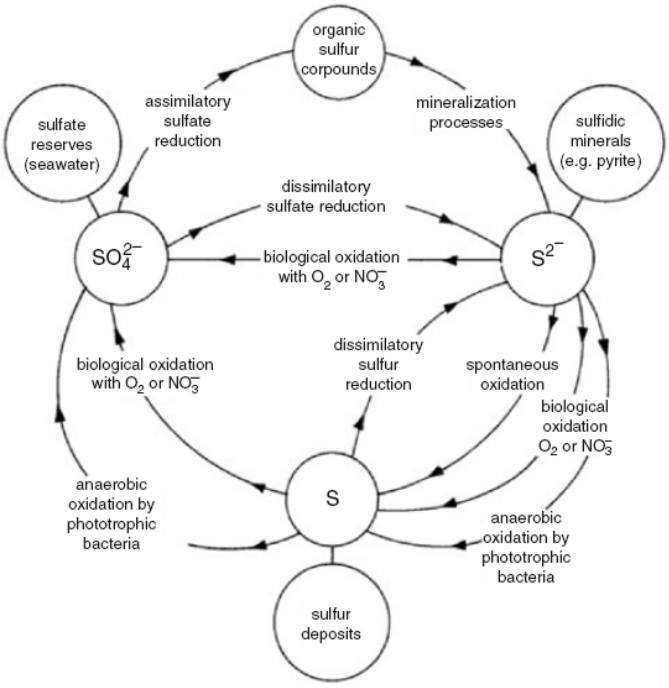

Figure 1.2. Sulfur cycle and associated oxidative and reductive processes that are both biologically and abioticlly mediated (reproduced with permission from Robertson and Kuenen 2006).

SOB can be divided into two groups, colorless or photosynthetic. The colorless bacteria are named due to their lack of photopigments and can use reduced sulfur compounds with oxygen or nitrate as a source of energy for growth (Robertson and Kuenen 2006). These organisms have been divided into four groups based on their organic/inorganic carbon and energy source requirements: obligate chemolithotrophs, facultative chemolithotrophs or mixotroph, chemolithoheterotroph, and chemoorganoheterotroph (Robertson and Kuenen 2006).

The microorganism studied in this project, *Bosea* sp. WAO, is a facultative chemolithotroph. These organisms can grow with an inorganic energy source and carbon dioxide, or with complex organic carbon that provides both carbon and

energy (Robertson and Kuenen 2006). Reduced sulfide produced by the reductive half of the sulfur cycle can bind various metals to produce metal sulfides. In extreme environments such as low pH or high temperatures, the ability of microorganisms to oxidize the sulfide bound in metal sulfides such as pyrite (FeS_2) and galena (PbS) have been extensively studied. At circumneutral pH, however, less is understood about microbial-mineral interactions (Bang *et al.*, 1995, Roberson and Kuenen 2006). This may be due to the complexity of separating biotic from abiotic processes at neutral pH conditions.

sox gene cluster. The *sox* gene cluster is a pathway consisting of seven essential genes, *soxXYZABCD*, that code for proteins required for the direct oxidation of sulfide to sulfate *in vivo* (Fig. 1.3) (Friedrich *et al.*, 2001). These proteins are localized to the periplasm in SOB (Friedrich *et al.*, 2001). Homologs of the proteins SoxA, SoxB, SoxY, and SoxZ have been determined from the available sequence data of SOB (Friedrich *et al.*, 2001). SoxXA consists of two *c*-type cytochromes which oxidatively couples the sulfane sulfur of the compound to the SoxY cysteine sulfhydryl group. SoxYZ then covalently binds the sulfur and chelates the compound, after which SoxB hydrolyzes the sulfonal sulfate from the thiocysteine-S-sulfate residue. Finally, $Sox(CD)_2$ oxidizes the remaining outer sulfur atom to sulfate (Friedrich *et al.*, 2001, Ghosh *et al.*, 2009). The cycle repeats until all sulfur molecules have been oxidized from the original starting compound and SoxYZ is reformed (Friedrich *et al.*, 2001, Ghosh *et al.*, 2009). Primers are available for *soxB* which have been used as an indicator for

thiosulfate oxidation ability (Meyer *et al*., 2007). This gene can be used as an indicator for the presence of other *sox* genes in SOB as they are typically found in a gene cluster (Meyer *et al*., 2007).

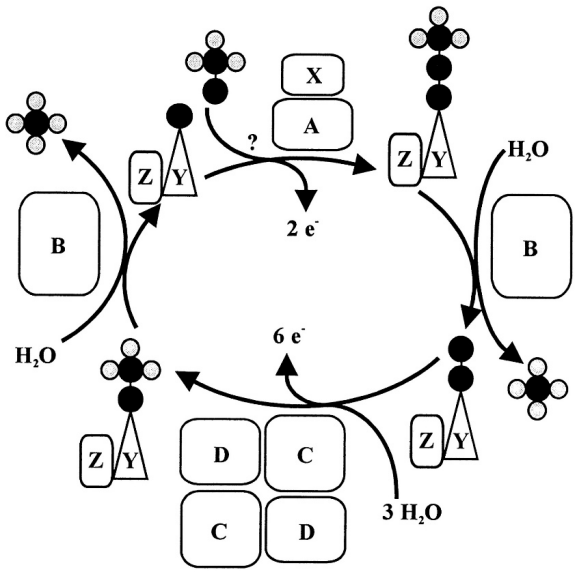

Figure 1.3. Model of the sulfur oxidation reactions of the sox pathway from the model organism *Paracoccus pantotrophus* (reproduced with permission from Friedrich *et al*., 2001). Black circles represent sulfur molecules and grey circles are oxygen molecules.

Microbiological Activity with Metals and Inorganic Sulfur. Study of microorganisms in relation to metals and sulfur has mostly been focused on mining systems related to the mining of economically important minerals and metals. Microorganism have long been implicated in the oxidation of inorganic sulfur compounds found in ore deposits leading to acid mine/rock drainage (Colmer and Hinkle 1947, Hoffert 1947, Nordstrom *et al*., 2015). Acid mine drainage (AMD) is caused by the exposure of sulfidic minerals to oxygen and groundwater leading to their oxidation producing sulfuric acid and waters heavily polluted with metals and metalloid contaminants especially iron (Hoffert 1947, Johnson and Hallberg 2005, Nordstrom *et al*., 2015). Pyrite (FeS_2) is the

dominant metal sulfide mineral and pyrite rich deposits are usually mined for Au, Ag, Cu, Zn, and Pb that can occur as impurities or as their own metal sulfides (Dudka and Adriano 1997, Baker and Banfield 2003). The bacterium *Acidothiobacillus ferroxidans*, previously named *Thiobacillus ferroxidans*, is the most well-known iron oxidizer, which oxidizes the ferrous iron bound in pyrite to ferric, while other microorganisms act on the sulfide (Taylor *et al*., 1984, Nordstrom *et al*., 2015). Microbial diversity studies have shown *Leptospirillium* and archaea are the dominate iron oxidizers near the primary waste source while a greater diversity of microorganisms are found as you move downstream into milder conditions (Baker and Banfield 2003, Majzlan *et al*., 2011, Nordstrom *et al*., 2015). Sulfur oxidizers in these communities are autotrophic and pure cultures demonstrating sulfur oxidation have been identified as *Acidothiobacillus ferroxidans*, *Thiobacillus thiooxidans*, *Sulfobacillus disulfidooxidans*, *Thiobacillus albertis* and *Sulfobacillus acidophilus* (Baker and Banfield 2003). Remediation of acid mine drainage sites utilize bacterial metabolism in systems such as: constructed aerobic wetlands where iron is oxidized to make it immobile; or installation of anaerobic bioreactors amended with organic carbon sources where reduction of iron and sulfur causes immobilization by precipitation and binding of additional contaminants (Johnson and Hallberg 2005, Nordstrom *et al*., 2015). Additionally, bacteria are used for bioleaching processes to recover trace metals from waste piles and low grade ore that may not have been economically favorable under the original mining conditions such as for gold, copper, and

uranium (Tributsch 2001, Mohapatra *et al.*, 2008). The sulfide ores are purposely placed in conditions to enhance microbial oxidation to remove sulfide and the leachate is captured and treated to remove soluble metals of interest (Mohapatra *et al.*, 2008).

Less studied neutral mine drainage occurs at sites where the mineral composition contains enough carbonates to react with and neutralize the sulfuric acid produced by oxidation of the sulfidic minerals (Ondrejkova *et al.*, 2013, Majzlan *et al.*, 2011, Frau *et al.*, 2015, Nordstrom *et al.*, 2015). Under neutral and weakly alkaline pH conditions arsenic and antimony can become more mobilized while the other metals such as iron, lead, zinc, copper, and gold will have reduced solubility (Ondrejkova *et al.*, 2013, Majzlan *et al.*, 2011, Frau *et al.*, 2015, Nordstrom *et al.*, 2015). Under weakly alkaline (pH ~8.5) conditions Sb and As form oxyanions that desorb from the negatively charged Fe(III) phases (Ondrejkova et al., 2013, Frau *et al.*, 2015). Additionally, at neutral pH strong reducing conditions occur and Fe and Mn oxides are reduced releasing the associated As and Sb (Smedley and Kinniburgh 2002, Nordstrom *et al.*, 2015).

Here I will focus on the oxidation of the electron donors: sulfur in the form of galena (PbS), arsenic in the form of arsenopyrite (FeAsS) and arsenic (III), and antimony in the form of stibnite (SbS_2), antimony (III), and antimony (0) under the less explored neutral conditions.

Lead. The trace heavy metal lead in galena (PbS) is released into the environment from anthropogenic sources including garbage dumps, mining

operations, and industrial processing (Taillefert *et al*., 2000). Global mine production of Pb was 5.5 million tons in 2013 with the United States' 14 mines accounting for 0.34 million tons and China the highest at 3.9 million tons (Guberman and USGS 2015a).

Lead exposure can result in slowed growth, hearing problems, headaches, and behavioral and learning problems (U.S. EPA 2008, Adadin *et al*., 2007). It also specifically targets the brain and nervous system (U.S. EPA 2008, Adadin *et al*., 2007). As a result, lead is especially harmful to children because they are still in the crucial stages of development. In adults it can cause reproductive problems, high blood pressure, hypertension, nerve disorders, memory and concentration problems, and muscle and joint pain (U.S. EPA 2008, Adadin *et al*., 2007).

The trace metal will bind to organic matter, clays, iron, and manganese-oxides when present in oxidizing conditions of overlaying water and oxic sediments. As reducing conditions increase, Pb will bind to sulfide to form the metal monosulfide galena (PbS) (Canavan *et al*., 2007). Sediment pore waters are usually supersaturated with PbS (Canavan *et al*., 2007). During sediment disturbance events oxygen can be mixed into the anoxic sediment and remobilize these metals by spontaneous or microbially mediated oxidation (Eggleton and Thomas 2004).

Phosphate Amendment. A common method for in place soil stabilization for Pb contamination involves the addition of phosphate to convert more soluble

Pb minerals to pyromorphite ($Pb_5(PO_4)_3X$) where X=Cl, F, Br, or OH (Ruby *et al.*, 1994, Zhang and Ryan 1999, Martinez *et al.*, 2004, Kumpiene *et al.*, 2008, Scheckel *et al.*, 2013). Secondary pyromorphite-type phases have low solubility and limited bio-accessibility compared to the primary Pb minerals (Kumpiene *et al.*, 2008). Furthermore, pyromorphite is not redox sensitive thus changing the long term mineral stability, particularly in soil environments subject to fluctuating water table levels. Galena (PbS) is a relatively insoluble Pb mineral with a $K_{sp} = 10^{-28.3}$ but when exposed to oxygen it becomes unstable and oxidizes to more soluble forms (Hsieh and Huang 1988, Ruby *et al.*, 1994). Addition of phosphate has been shown to react with the mineral and form pyromorphite which is more stable at ambient oxidizing surface conditions (Zhang and Ryan 1999). In an acid mine drainage situation, the addition of phosphate as apatite from fish bone has been shown to both bind metals and buffer the water pH to neutral conditions (Oliva *et al.*, 2011).

Previous studies examining microbial activity in relation to soil amendments has focused on utilizing microbes to increase the solubility of phosphate amendments to enhance the reaction with Pb (Park *et al.*, 2011, Wilson *et al.*, 2006, Park and Bolan 2013). These bacteria have been shown to release organic acids that decrease pH and increase the solubility of rock phosphate (Park *et al.*, 2011). Phosphate solubilizing bacteria (PSB) have been shown to enhance the reaction of insoluble phosphates with Pb in soil and agar medium (Park and Bolan 2013). A combination of different organisms with three

types of phosphate amendments caused a decrease in Pb availability (Wilson *et al.*, 2006). To date, very little is known about how microorganisms might be able to use the reduced sulfur for chemolithoautotrophic growth during these phosphate amendments. Since S is a key nutrient for microbial growth I hypothesize that the reaction of phosphate with PbS would provide bioavailable sulfur for chemolithoautotrophic growth.

Arsenic. Arsenic is a naturally occurring metalloid in Group 15 of the Periodic Table of Elements, just below phosphorus. It is abundant in the Earth's crust ranging between 1.0-2.5 mg/kg and is a component of over 200 minerals (Matschullat 2000, Mandal and Suzuki 2002, Bowell *et al.*, 2014). Arsenic has four possible oxidation states -3, 0, +3, and +5 and is interesting because it is capable of existing in both anionic and cationic forms (Holleman and Wiberg 2001c, Bissen and Frimmel 2003). Arsenic occurs most commonly as the minerals: arsenopyrite (AsFeS), realgar (As_2S_4), orpiment (As_2S_3), and as the weathering product arsenic trioxidie (As_2O_3) (Matschullat 2000, Holleman and Wiberg 2001c, Mandal and Suzuki 2002). It can also occur with other metals as the form M(II)AsS with M(II)=Ni, Co, and Pb (Matschullat 2000, Mandal and Suzuki 2002). In settings where there are high concentrations of soluble As(III) and sulfide a precipitation reaction will occur to form the sulfide minerals AsFeS, As_2S_4, and As_2S_3 (Smedley and Kinniburgh 2002). World production of arsenic in 2013 was 45,200 metric tons with China leading production with 25,000 metric tons (Edelstein and USGS 2015). The United States stopped domestic production

of arsenic trioxide and primary arsenic metal in 1985; however, some areas of the United States have naturally high levels of arsenic contamination in the groundwater due to mineral dissolution and weathering (Edelstein and USGS 2015).

Arsenic has been released into the environment due to anthropogenic activities such as the combustion of fossil fuels, smelting, cement work, electronics, wood preservatives, pesticides, herbicides, semiconductors, alloys for gunshot, and wastes from animal husbandry where it is used in feed and as a disinfectant (Matschullat 2000, Holleman and Wiberg 2001c, Mandal and Suzuki 2002, Bowell *et al*., 2014). It is also released into the environment by natural processes such as rock weathering and volcanic activity (Bissen and Frimmel 2003, Bowell *et al*., 2014). The U.S. EPA considers arsenic a group I carcinogen and a pollutant of primary concern with drinking water limits set at 10 µg/L (Ng *et al*., 2001, Mandal and Suzuki 2002). Arsenic is taken up into the human body by phosphate transporters [As(v)] and aquaglyceroporin channels [As(III)] (Bowell *et al*., 2014). Health problems are caused by both acute and long term exposure that can affect all major body systems (Mandal and Susuki 2002). Long term exposure causes arsenicosis which includes skin lesions and skin cancer (Ng *et al*., 2003). Inorganic As(III) is considered more toxic and mobile than As(V); however, both are absorbed quickly through the lungs and intestines but not as readily through the skin (Matschullat 2000, Mandal and Suzuki 2002).

Microorganisms affect the fate and transport of arsenic by changing the redox speciation of arsenic and arsenic compounds in the environment (Kang *et al*., 2012). They are able to reduce, oxidize, methylate, and demethylate arsenic compounds both for energy production and detoxification (Silver and Phung 2005, Ehrlich and Newman 2008b, Amend *et al*., 2014). There are over 200 organisms that have been identified as able to either oxidize or reduce arsenic and "within the Bacteria, they identify as Aquificae, Deinococcus-Thermus, Chloroflexus, Firmicutes, Actinobacteria, Deferribacteres, Chrysiogenetes, Cyanobacteria, Proteobacteria (including members of the α, β, γ, δ, and ε subgroups), and Bacteroidetes" (Amend *et al*., 2014). Based on differences in metabolism the organisms can be divided into four groups: dissimilatory arsenate reducing prokaryotes, arsenite resistant microorganisms, chemoautotrophic arsenite oxidizers, and lastly heterotrophic arsenite oxidizers (Silver and Phung 2005, Lett *et al*., 2012, Amend *et al*., 2014). The dissimilatory arsenate reducing prokaryotes require the genes *arrAB* for metabolic energy gaining reactions from the reduction of As(V) to As(III) (Silver and Phung 2005, Amend *et al*., 2014). For detoxification organisms use the gene *arsC* which couples the reduction of As(V) to As(III) and subsequent transport out of the cell (Silver and Phung 2005, Amend *et al*., 2014). Aerobic arsenite oxidation occurs using the *aio* genes renamed from *aso*, *aro* and *aox* all formerly used in different organisms (Lett *et al*., 2012). The *aioA* encodes for a large molybdopterin containing subunit with a guanosine dinucleotide at the active site and *aioB* encodes for a small Rieske

subunit (Silver and Phung 2005, Lett *et al*., 2012, Amend *et al*., 2014). This pathway also has a two component regulatory system that includes a sensor histidine kinase gene, *aioS* (*aoxS*, *aroS*) and a transcriptional regulator gene, *aioR* (*aoxR*, *aroR*) (Silver and Phung 2005, Lett *et al*., 2012, Amend *et al*., 2014). Anaerobic arsenite oxidation occurs using the *arxAB* genes which are used by two types of organisms: those that can obtain energy by anaerobic respiration with nitrate and those that can use anoxygenic photosynthesis with As(III) as the e-donor (Amend *et al*., 2014). The many ways microorganisms can utilize arsenic and arsenic containing compounds for their metabolism suggests these organisms play an important role in the biogeochemical cycling of this element.

Antimony. Antimony is a naturally occurring rare earth element in Group 15 of the Periodic Table of Elements, just below arsenic. It has four possible oxidation states -3, 0, +3, and +5. In the environment antimony is predominately found as its ore stibnite (Sb_2S_3) and valentinite (Sb_2O_3) an oxidation product (Filella *et al*. 2002). World mine production of antimony was 154,000 metric tons in 2013 with China producing the most at 120,000 metric tons (Guberman and USGS 2015b). In the United States in 2014 "distribution of primary antimony consumption was as follows: nonmetal products, including ceramics and glass, and rubber products, 42 %; flame retardants, 32 %; and metal products, including antimonial lead and ammunition, 26 %" (Guberman and USGS 2015b).

Due to anthropogenic activities antimony at the Earth's surface has been enriched by an order of 70 times (Filella *et al*., 2002). Antimony was historically used in cosmetics and is now used in semiconductors, in alloys of lead and tin, in therapeutic agents for tropical diseases and increasingly in flame retardants (Holleman and Wiberg 2001a, Filella *et al*., 2002). The increased utilization in flame retardants has reduced the amount of antimony that is recoverable and reused, increasing the potential for environmental contamination (Filella *et al*., 2002). Stibnite is specifically used in the production of matches, munitions, fireworks, ruby glass, and dyes for plastics (Holleman and Wiberg 2001a). The U.S. EPA considers antimony a pollutant of priority interest and has set a maximum contaminant limit in drinking water of 6 µg/L (Filella *et al*., 2002). However, since antimony is used as a therapeutic agent for tropical protozoan diseases such as leishmaniasis, schistosomaiasis, ascariasis, trypanosomasis, and bilhaeziasis most toxicity work focuses on medical dosages levels and not levels that would be seen in the natural environment (Filella *et al*., 2002).

The majority of studies on microbial interactions with antimony have focused on organisms tolerant to mining area conditions with low pH or utilized the soluble compound potassium antimonyl tartrate. Torma and Gabra (1977) show that *Thiobacillus ferrooxidans* (renamed *Acidothiobacillus ferrooxidans*) was able to optimally oxidize the sulfur in stibnite to sulfate at pH 1.75 and 35 °C. They also showed that 5-7 % of the antimony was oxidized from Sb(III) to Sb(V) but could not confirm if the antimony oxidation was due to direct microbial

activity (Torma and Gabra 1977). Other organisms isolated on antimony sulfide ore in acidic environments have shown that the organisms grow and can oxidize the sulfur but the fate of the antimony is unclear (Tsaplina *et al.*, 2010, Zhuravleva *et al.*, 2011). Additionally, microbes have shown resistance to antimony by removing Sb(III) using efflux pumps such as the ArsB protein, Acr3p family, and the ABC (ATP-binding cassette) transporter (Filella *et al.*, 2007). Both ArsB and Acr3p have previously been shown to be involved in arsenic resistance (Filella *et al.*, 2007). Studies using potassium antimonyl tartrate have shown that Sb(III) resistant bacteria are capable of oxidizing the Sb(III) to Sb(V) and that growth was observed during this activity (Lehr *et al.*, 2007, Li *et al.*, 2013). Additional studies are necessary to continue to elucidate if antimony can be used as an electron donor for growth.

Model Organism. Bosea sp. WAO (White Arsenic Oxidizer) is a novel strain of the genus *Bosea* in the family *Bradyrhizobiaceae* that was isolated from an enrichment culture amended with arsenite and inoculated with pulverized pyrite shale. This organism is a facultative chemolithoautotroph that can grow at neutral pH with inorganic energy sources and carbon dioxide, or with complex organic carbon that provides both carbon and energy (Rhine *et al.*, 2008). The *Bosea* genus is within the class *Alphaproteobacteria* and family *Bradyrhizobiaceae* which currently consists of 12 genera: *Bradyrhizobium*, *Afipia*, *Agromonas*, *Balneimonas*, *Blastobacter*, *Bosea*, *Nitrobacter*, *Oligotropha*, *Rhodoblastus*, *Rhodopseudomomonas*, *Salinarimonas*, and *Tardiphaga*

(Marcondes de Souza *et al.,* 2014). These organisms have been isolated from diverse environments including soils, plants, and animal hosts (Marcondes de Souza *et al.,* 2014). Within the genus *Bosea* there are nine species with validly published names: *B. thiooxidans* BI-42^T (AF508803) from agricultural soil (Das *et al.,* 1996) *B. eneae* 34614^T (AF288300), *B. vestrisii* 34635^T (AF288306), and *B. massiliensis* 63287^T (AF288309) were isolated from a hospital water system (La Scola *et al*., 2003), *B. minatitlanensis* AMX51^T (AF273081) isolated from anaerobic digester sludge (Ouattar *et al.,* 2003) and *B. lupini* R-45681^T (FR774992), *B. lathyri* R-46060^T (FR774993), and *B. robiniae* R-46070^T (FR774994) were isolated from the root nodules of legumes (De Meyer *et al.,* 2012) and *B. vaviloviae* Vaf-18^T from the root nodules of *Vavilovia Formosa* (Safronova *et al*., 2015). Ten genome sequences of *Bosea* spp. are publicly available of which four are validly named and characterized to species level: *B. thiooxidans* CGMCC 9174 V5_1, *B. lathyri* DSM 26656^T, *B. lupini* DSM 26673^T, *B. vaviloviae* strain SD260 and six uncharacterized: *Bosea* sp. 117, *Bosea* sp. UNC402CLCol, *Bosea* sp. LC85, *Bosea* sp. OK403, *Bosea* sp. AAP35, and *Bosea* sp. AAP25. Only *B. thiooxidans* CGMCC 9174 V5_1 and *B. vaviloviae* strain SD260 have whole genome sequences available in GenBank. The ability of the characterized organisms *Bosea lathyri* and *Bosea lupini* to oxidize thiosulfate has not been determined (De Meyer and Willems 2012).

Growth under heterotrophic and chemolithoautotrophic conditions was tested with a number of substrates and published in Rhine *et al*. 2008. *Bosea* sp.

WAO can grow heterotrophically on defined medium with acetate, glucose, and lactate. *Bosea* sp. WAO will also grow in the complex media trypticase soy broth, yeast extract, and nutrient broth. Autotrophically *Bosea* sp. WAO can grow on carbon dioxide with the soluble electron donors arsenite, thiosulfate, and polysulfide. Additionally, this organism can grow on the insoluble substrates elemental sulfur and arsenopyrite (FeAsS). This organism's flexible metabolism and ability to utilize soluble and insoluble electron donors made it an excellent choice for additional work on microbe mineral interactions. (Rhine *et al.*, 2008)

Study Scope and Objectives

The main goal of this study was to explore microbe-mineral interactions at circumneutral pH by (i) utilizing the model organism *Bosea* sp. WAO to understand the metabolism and selected functional genes involved in these processes (ii) to look at a variety of electron donors that are both soluble and insoluble compounds. To accomplish these goals, the genome of *Bosea* sp. WAO was sequenced and annotated to identify functional genes of interest. Experimental work exploring the transformation of PbS and release of sulfur as a bioavailable electron donor and in addition to studies with the alternative electron donors Sb(0), Sb(III), and Sb_2S_3 were conducted.

Specific Objectives:

1. To explore the genome of *Bosea* sp. WAO and specifically identify genes for sulfur and arsenic metabolism.

2. To determine the fate of sulfur when phosphate is used as a remediation technique for galena (PbS) contamination in the presence and absence of *Bosea* sp. WAO.
3. To determine *Bosea* sp. WAO's ability to elemental antimony, potassium antimonyl tartrate, and stibnite (Sb_2S_3) for growth. Additionally, to look at the ability of three other sulfur oxidizing microorganisms to utilize the alternative electron donors elemental antimony and potassium antimonyl tartrate oxidation for growth.

Chapter 2:

Characterization and Draft Genome Sequence of *Bosea* sp. WAO

Abstract

Bosea sp. WAO is a novel strain of the genus *Bosea* in the family *Bradyrhizobiaceae*. *Bosea* sp. WAO was isolated from pulverized pyritic shale containing elevated levels of arsenic. This aerobic microorganism is capable of facultative chemoautotrophic growth by oxidizing arsenite, elemental sulfur, thiosulfate, polysulfide, and amorphous sulfur. This organism is able to grow optimally at 25 °C and pH 8 with intolerance to salinity above 3.5 % w/v NaCl. Genome analysis revealed that in addition to containing the arsenite oxidase genes for the large and small subunit, *aioA* and *aioB*, strain WAO also possesses the complete sulfur oxidation pathway which oxidizes thiosulfate fully to sulfate. The draft genome is of a single circular chromosome 6,125,776 bp long consisting of 21 scaffolds with a G+C content of 66.84 %. A total 5,727 genes were predicted of which 5,665 or 98.92 % are protein-coding genes and 62 RNA genes.

Introduction

Bosea sp. WAO (white arsenic oxidizer) was enriched from a pulverized sample of weathered black shale obtained from an outcrop near Trenton, NJ that contained high levels of arsenic (Rhine *et al.*, 2008). Strain WAO belongs to the class *Alphaproteobacteria* and family *Bradyrhizobiaceae* which currently consists

of 12 genera: *Bradyrhizobium*, *Afipia*, *Agromonas*, *Balneimonas*, *Blastobacter*, *Bosea*, *Nitrobacter*, *Oligotropha*, *Rhodoblastus*, *Rhodopseudomomonas*, *Salinarimonas*, and *Tardiphaga* (Marcondes de Souza *et al*., 2014). This phenotypically diverse family is composed of microorganisms that are involved in nitrogen cycling, human diseases, phototropism in non-sulfur environments, plant commensalism, and chemolithoautotrophic growth (Marcondes de Souza *et al*., 2014). 16S rRNA gene analysis of the *Bradyrhizobiaceae* family indicates that the *Bosea* genus is most closely related to the genus *Salinarimonas* which currently consists of two species, *S. rosea* and *S. ramus* (Marcondes de Souza *et al*., 2014).

The microorganisms belonging to the genus *Bosea* have been isolated from a variety of environments such as soils, sediments, hospital water systems, and digester sludge (Das *et al*., 1996, La Scola *et al*., 2003, Ouattara *et al*., 2003). The type strain *Bosea thiooxidans* BI-42^{T} is capable of thiosulfate oxidation and the initial genus definition included this characteristic (Das *et al*., 1996). In 2003 La Scola emended the genus description to remove thiosulfate oxidation as a key descriptor after isolation of several other *Bosea* spp. that were unable to oxidize thiosulfate (La Scola *et al*., 2003). These organisms have a very diverse metabolism but their common characteristics include being Gram-negative, aerobic, rod shaped, motile, good growth between 25 to 35 °C, intolerant to salt concentrations above 6 % NaCl and have been described to be heterotrophic (Das *et al*., 1996, La Scola *et al*., 2003, Ouattara *et al*., 2003).

Using selective enrichment and isolation techniques with arsenite [As(III)] as the sole electron donor, *Bosea* sp. WAO, was isolated under autotrophic conditions (Rhine *et al*., 2008). Here I summarize the physiological features together with the draft genome sequence and data analysis of *Bosea* sp. WAO.

Materials and Methods

Genome project history. *Bosea* sp. WAO was selected for sequencing based on the organism's ability to grow both heterotrophically and chemolithoautotrophically with arsenite and reduced sulfur compounds. Sequencing and assembly was completed at the Rutgers School of Environmental and Biological Sciences Genome Cooperative. A paired-end library was constructed using an Illumina Nextera Kit and sequenced using an Illumina Genome Analyzer IIX (Illumina Inc., San Diego, CA). The sequence assembly was performed using the CLC Genomics Workbench 5.1 (CLC Bio, Cambridge, MA). The draft genome was submitted to NCBI Whole Genome Shotgun (WGS) and also to the JGI Integrated Microbial Genomes/ Expert Review (IMG/ER). A summary of the project is shown in Table 2.1.

Growth conditions and genomic DNA preparation. A culture of *Bosea* sp. WAO, GeneBank: DQ986321.1, was grown in a dilute (50 % normal strength) trypticase soy broth amended with 5 mM sodium arsenite and 5 mM sodium thiosulfate and incubated in the dark at 30 °C on an orbital shaker for maximum

oxygen exchange. Genomic DNA was extracted using the MoBio Powersoil Kit following manufacturer's directions with the modification that DNA was eluted into 100 uL water instead of buffer.

Genome sequencing and assembly. A paired-end library was constructed using an Illumina Nextera Kit and sequenced using an Illumina Genome Analyzer IIX (Illumina Inc., San Diego, CA). The sequence assembly was performed using the CLC Genomics Workbench 5.1 (CLC Bio, Cambridge, MA). An average coverage of 240x and a mean read length of 106 bp was obtained. The genome was assembled into 42 contigs with no additional gap closures.

Genome annotation. Genes were identified using the standard operating procedures of the DOE-JGI Microbial Genome Annotation pipeline (Markowitz *et al*., 2012) and The RAST Server: Rapid Annotation using subsystem technology (Overbeek *et al*., 2005, Aziz *et al*., 2008). JGI-IMG/ER was used to obtain COG identities and overall statistics of the genome. RAST was used to identify functional genes of interest involved in sulfur and arsenic metabolism.

Physiological characterization. The growth range and optimum conditions for temperature, pH, and salinity were completed in trypticase soy broth. Growth was measured by monitoring the change in OD of triplicate cultures for each variable at 625 nm in comparison to a respective media control. The effect of temperature on growth was determined from 20 - 45 ºC at 5 ºC increments. The effect of pH was determined at 10 pH values from 4.5 - 9 pH increasing by 0.5 pH increments. Media pH was adjusted by adding in either sodium hydroxide or

hydrochloric acid to obtain desired pH and then autoclaved before usage. The affect of salinity was measured at eight concentrations from 0.5 – 15.5 % weight/volume of sodium chloride added to the medium. For both the pH and salinity experiments cultures were kept at 30 °C in the dark on an orbital shaker for maximal air exchange.

Results and Discussion

Classification. The genus *Bosea* has nine species with validly published names: *B. thiooxidans* BI-42^T (AF508803) from agricultural soil (Das *et al*., 1996), *B. eneae* 34614T (AF288300), *B. vestrisii* 34635T (AF288306), and *B. massiliensis* 63287T (AF288309) were isolated from a hospital water system (La Scola *et al*., 2003), *B. minatitlanensis* AMX51T (AF273081) isolated from anaerobic digester sludge (Ouattara *et al*., 2003) and *B. lupini* R-45681T (FR774992), *B. lathyri* R-46060T (FR774993), and *B. robiniae* R-46070T (FR774994) were isolated from the root nodules of legumes (De Meyer *et al*., 2012), and *B. vaviloviae* Vaf-18^T from the root nodules of *Vavilovia formosa* (Safronova *et al*., 2015). The highest 16S rRNA pairwise similarities for strain WAO were found with the type strains *B. vestrisii* 34635^T (99.72 %), *B. eneae* 34614^T (99.65 %), *B. lupini* R-45681^T (99.65 %), *B. thiooxidans* BI-42^T (99.24 %), *B. robiniae* R-46070^T (98.88 %), *B. massiliensis* 63287^T (98.81 %), *B. minatitlanensis* AMX51^T (98.48 %) and *B. lathyri* R-46060^T (98.18 %) (Kim *et al*., 2012). Phylogenetic analysis based on the 16S rRNA gene of *Bosea* spp. and

phylogenetically related organisms placed *Bosea* sp. WAO closest to the type strain *B. lupini* DSM 26673^T with *B. vestrisii* 34635^T and *B. eneae* 34614^T in the same cluster (Fig. 2.1, Table 2.2). An average nucleotide identity analysis (ANI) score between strain WAO and *B. lupini* DSM 26673^T was 84.64 % computed using IMG/ER (Markowitz et al., 2012). This value is lower than the ANI species demarcation threshold range (95-96 %) (Kim *et al*., 2014). The ability of *B. lupini* to oxidize thiosulfate has not been determined (De Meyer *et al*., 2012); however, both *B. vestrisii* 34635^T and *B. eneae* have been determined to not oxidize thiosulfate to sulfate (La Scola *et al*., 2003). These results suggest that strain WAO represents a distinct species in the genus *Bosea*.

Morphology and Physiology. *Bosea* sp. WAO is Gram-negative, strictly aerobic, motile and rod shaped. Colonies on trypticase soy agar grow as large as 10 mm after 2 weeks at 30 °C and are smooth, mucoid, round, convex, and beige. Colonies on minimal salts medium supplemented with 5 mM sodium thiosulfate only grow to a diameter of 2 mm after 2 weeks at 30 °C and are smooth, round, and white. Growth occurs at a temperature range between 20 – 35 °C, optimally at 25 °C (Fig. 2.2). *Bosea* sp. WAO grows at pH 6 - 9, optimally at pH 8, while at more acidic pH values below 5.5 there is a significant delay in exponential growth phase with no growth below pH 4.5 (Fig. 2.3). Growth over a range of salinities was tested with no growth observed over 3.5 % w/v NaCl (Fig. 2.4). Cells will grow freely floating or attached to a mineral surface as shown in Figure 2.5.

Strain WAO is a strict aerobe that can grow heterotrophically on acetate, glucose, and lactate in addition to autotrophically on carbon dioxide with the electron donors arsenite, thiosulfate, polysulfide, and elemental sulfur. The organism is also able to grow on the mineral arsenopyrite (FeAsS) by oxidizing both the arsenic and sulfur to produce sulfate and arsenate. No growth was observed under aerobic conditions with the aromatic compounds phenol, benzoate, or ferulic acid; or with the electron donors sulfite, ammonium, nitrite, selenite, or chromium(III) (Rhine *et al*., 2008).

Bosea spp. *Genome Comparisons*. Ten other genome sequences of *Bosea* spp. are publicly available of which four down to species are validly named and characterized: *B. thiooxidans* strain CGMCC 9174 V5_1, *B. lathyri* DSM 26656^T, *B. lupini* DSM 26673^T, *B. vaviloviae* strain SD260 and six uncharacterized: *Bosea* sp. 117, *Bosea* sp. UNC402CLCol, *Bosea* sp. LC85, *Bosea* sp. OK403, *Bosea sp*. AAP35, and *Bosea sp*. AAP25. Only *B. thiooxidans* strain CGMCC 9174 V5_1 and *B. vaviloviae* strain SD260 have whole genome sequences available in GenBank. Table 2.5 details the basic characteristics of the ten genomes. The genomes range in size from 4.4 Mb to 6.6 Mb and G+C content between 64 to 68 %, a predicated gene number range from 3984 to 6267. *Bosea sp*. WAO's genome size (6.1 Mb), number of predicted genes (5727), number genes with function (4570), and number placed in COGs (4193) are all higher than the average for the draft genomes. However, both the percentage values for genes with functional predication (79.8 %) and percentage in COGs (73.2 %) are similar to

the average values for the draft genomes. *B. thiooxidans* CGMCC 9174 V5_1, *B. vaviloviae* strain SD260, *Bosea* sp. 117 and *Bosea* sp. UNC402CLCol contain pseudo genes. None of the IMG database genomes have been finished with scaffold numbers ranging between 16 and 72.

Insights from the Genome: *Arsenite Oxidation*. *Bosea* sp. WAO is able to grow under chemolithoautotrophic conditions with arsenite in addition to growing under heterotrophic conditions. Metabolic studies indicated that the organism was able to stoichiometrically oxidize the electron donors As(III) to As(V). Aerobic arsenite oxidation occurs using the *aio* genes renamed to reduce confusion from *aso*, *aro* and *aox*, which were formerly used to identify these genes in different organisms (Lett *et al*., 2012). AioA is a large molybdopterin containing subunit with a guanosine dinucleotide at the active site and AioB is a small Rieske subunit (Silver *et al*. 2005, Lett *et al*., 2012, Amend *et al*., 2014). This pathway also has a two component regulatory system that includes a sensor histidine kinase *aioS* (*aoxS*, *aroS*) and a transcriptional regulator *aioR* (*aoxR*, *aroR*) (Silver *et al*. 2005, Lett *et al*., 2012, Amend *et al*., 2014). For the initial publication of *Bosea* sp. WAO, only the large subunit gene for the arsenite oxidation pathway *aioA* (EF015463) was amplified by traditional PCR (Rhine *et al*., 2007, Rhine *et al*., 2008). Analysis of the genome herein revealed that the arsenite oxidation pathway was complete with *Bosea* sp. WAO possessing the small subunit *aioB* and reconfirming the large subunit *aioA* in addition to the remaining genes in the pathway. Of the available genomes only *Bosea* sp. WAO,

and *Bosea* sp. 117 genomes contain both the large and small arsenite subunits with amino acid similarities of 78 % for AioA and 73 % for AioB. The genes within the arsenite oxidation operon are in the same order (Fig. 2.6). The operon begins with a sensor histidine kinase, *aioS*, followed by a transcriptional response regulator, *aioR*, and then *aioB*, followed by *aioA*.

Insights from the Genome: *Reduced Sulfur Compound Oxidation. Bosea* sp. WAO is also able to grow under chemolithoautotrophic conditions with thiosulfate, polysulfide, and elemental sulfur. Metabolic studies indicated that the organism is able to stoichiometrically oxidize the electron donor S_2O_3 to SO_4^{2-}. The *sox* gene cluster is a pathway consisting of seven essential genes, *soxXYZABCD,* that code for proteins required for direct oxidation from sulfide to sulfate *in vivo* (Friedrich *et al*., 2001). The genome analysis indicated strain WAO possesses *soxB*, *soxX*, *soxY*, *soxZ*, *soxA*, *soxC*, and *soxD*, genes necessary in the sulfur oxidation pathway to allow for complete oxidation of S_2O_3 to SO_4^{2-}. *Bosea* sp. WAO, in addition to five other strains, *B. thiooxidans* CGMCC 9174 V5_1, *Bosea* sp. 117, *Bosea* sp. LC85, and *B. lupini* contain the complete *sox* system. For the four genomes available in IMG the overall gene order in the operons are the same for all organisms; however, *Bosea* sp. WAO and *B. lupini* have *soxA* and *soxX* on the plus strand and *soxY*, *soxZ*, *soxB*, *soxC*, *soxD* on the minus strand (Fig. 2.7). While *Bosea* sp. 117 and *Bosea* sp. LC85 have the genes on the reverse strands with *soxY*, *soxZ*, *soxB*, *soxC*, *soxD* on the plus and *soxA* and *soxX* on the minus strand (Fig. 2.7). Comparison of the translated nucleotide

sequence of *soxB* from *Bosea* sp. WAO to the translated *soxB* of the other five organisms showed that the protein sequence is 90 % similar to *Bosea* sp. LC85, 88 % similar to *B. lupini* and *B. thiooxidans* CGMCC 9174 V5_1, and 70 % similar to *Bosea* sp. 117. The presence of all the genes in the same order suggests these other strains in addition to the experimentally confirmed type strain *Bosea thiooxidans* BI-42^{T}, may be able to perform thiosulfate oxidation.

Insights from the Genome: *Additional Metabolic Pathways.* The Calvin Cycle consists of 13 enzymatic reactions with the enzyme ribulose-1,5 bisphosphate carboxylase/oxygenase (RuBisCO) responsible for the carbon fixation step (Shively et al., 1998). For the initial publication of *Bosea sp*. WAO the type II ribulose-1,5 bisphosphate carboxylase/oxygenase (RuBisCO) was amplified by traditional PCR (Rhine *et al*., 2007, Rhine *et al*., 2008). Analysis for the remaining genes of the Calvin-Benson-Bassham Cycle for carbon fixation indicated that all of the other required genes were present for carbon fixation to occur. Nine of the available genomes have a match for strain WAO's ribulose 1,5-bisphosphate carboxylase amino acid sequence: *B. thiooxidans* CGMCC 9174 V5_1, (85 %), *B. lathyri* DSM 26656^{T}, (86 %), *B. lupini* DSM 26673^{T}, (82 %), *B. vaviloviae* strain SD260, (85 %), *Bosea* sp. 117, (72 %), *Bosea* sp. UNC402CLCol, (85 %), *Bosea* sp. LC85, (84 %), *Bosea* sp. OK403, (87 %), and *Bosea sp*. AAP35, (84 %). Since RuBisCO is considered a biomarker for the Calvin Cycle this suggests carbon fixation may be widespread in this genus despite the limited experimental evidences.

Additional KEGG analysis indicated incomplete pathways for nitrogen reduction. *Bosea* sp. WAO possesses some genes for each of the reductive pathways but each is incomplete supporting the observation that no growth occurred when nitrate was provided as an electron acceptor. No genes involved in ammonia oxidation were identified again supporting the absence of growth when cultivated under those conditions (Rhine *et al.*, 2008). Using IMG/ER Pipeline analysis *Bosea sp*. WAO was determined to be prototrophic for L-aspartate, L-glutamate, and glycine; auxotrophic for L-lysine, L-alanine, L-phenylalanine, L-tyrosine, L-tryptophan, L-histine, L-arginine, L-isoleucine, L-leucine, and L-valine; and not to be able to synthesize selenocysteine or biotin based on the draft of the genome (Markowitz *et al.*, 2012). Using the SEED viewer *Bosea sp*. WAO has complete pathways for the: tricarboxylic acid cycle, pentose phosphate pathway, acetyl-coA acetogenesis pathway, methylglyoxal metabolism, dihydroxyacetone kinases, catechol branch of beta-ketoadipate pathway, glycerol and glycerol-3-phosphate uptake and utilization, D-ribose utilization, deoxyribose and deoxynucleoside catabolism, and lactate utilization.

COG analysis for *Bosea* sp. WAO assigned a large number of genes to amino acid transport and metabolism (13.76 %), transcription (8.13 %), inorganic ion transport and metabolism (8.06 %), and energy production and conservation (6.97 %). *Bosea* sp. WAO has 53 genes encoding for cytochromes alone. The number and percentage of genes associated with all COG functions is reported in Table 2.4.

Conclusions

Bosea sp. WAO is able to grow chemolithoautotrophically on both arsenite and reduced sulfur compounds. It was originally enriched from pyritic shale obtained from an outcropping containing arsenic in the Lockatong geological formation in the Newark Basin near Trenton, New Jersey (Rhine *et al.*, 2008). The draft genome consists of one circular chromosome containing 6.1 Mbps and a GC content of 68.84 %. Strain WAO is able to engage in the oxidative part of biogeochemical cycling and grow autotrophically when nutrient conditions are low. When conditions favor heterotrophic growth, however, the organism is able to rapidly increase in biomass and maintain its population under the varying conditions that are expected to prevail at an oxic mineral surface.

Tables and Figures

Table 2.1. Project information.

MIGS ID	Property	Term
MIGS 31	Finishing quality	Draft
MIGS-28	Libraries used	One pair-end
MIGS 29	Sequencing platforms	Illumina Genome Analyzer IIX
MIGS 31.2	Fold coverage	240x
MIGS 30	Assemblers	CLC Genomics Workbench 5.1
MIGS 32	Gene calling method	Glimmer
	Locus Tag	DK26
	Genbank ID	JXTJ00000000
	GenBank Date of Release	January 8, 2016
	GOLD ID	Gp0113237
	BIOPROJECT	PRJNA243637
MIGS 13	Source Material Identifier	
	Project relevance	Environmental, biogeochemical cycling of arsenic and sulfur

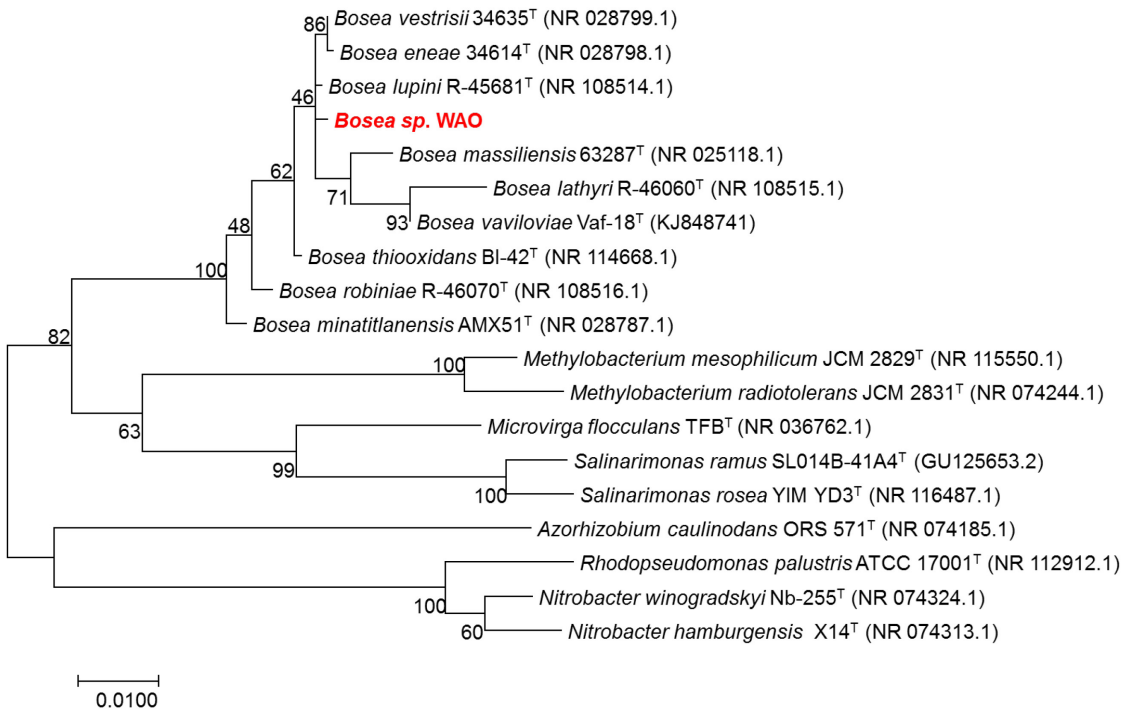

Figure 2.1. Molecular Phylogenetic analysis by Maximum Likelihood method tree highlighting the position of *Bosea* sp. WAO relative to the other *Bosea* spp using 16s rRNA. The evolutionary history was inferred by using the Maximum Likelihood method based on the Tamura-Nei model (Tamura and Nei 1993). The tree with the highest log likelihood (-4792.5378) is shown. The percentage of trees in which the associated taxa clustered together is shown next to the branches. Initial tree(s) for the heuristic search were obtained automatically by applying Neighbor-Join and BioNJ algorithms to a matrix of pairwise distances estimated using the Maximum Composite Likelihood (MCL) approach, and then selecting the topology with superior log likelihood value. The tree is drawn to scale, with branch lengths measured in the number of substitutions per site. The analysis involved 19 16S rRNA nucleotide sequences. All positions containing gaps and missing data were eliminated. There were a total of 1376 positions in the final dataset. Evolutionary analyses were conducted in MEGA7 (Kumar *at al.*, submitted).

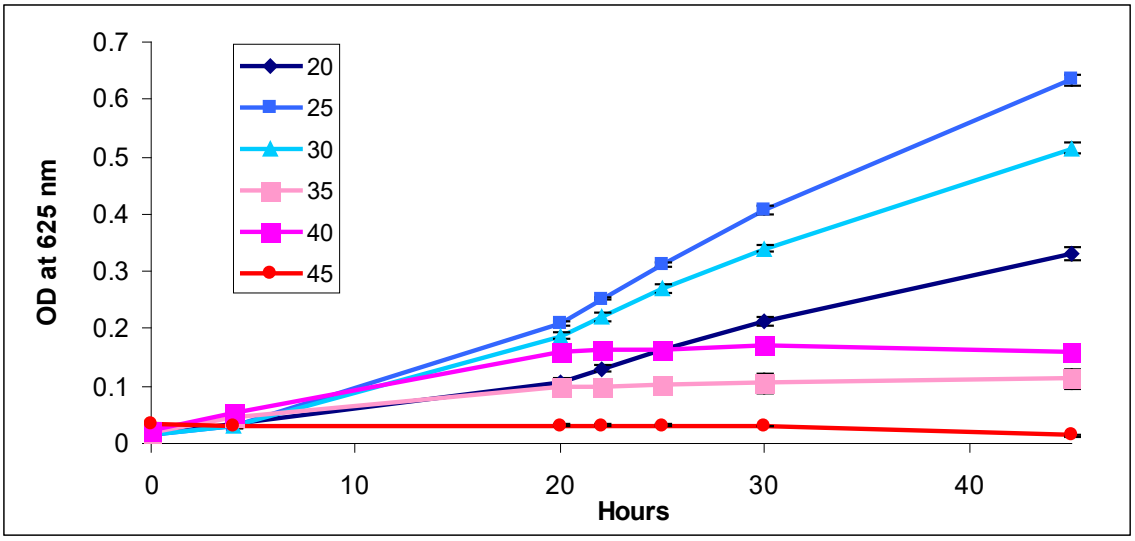

Figure 2.2. Growth of *Bosea* sp. WAO at six temperatures was determined by monitoring the change in OD at 625 nm in trypticase soy broth. Temperature ranged from 20- 45 ºC at 5 ºC increments. Each point represents three replicates with error bars representing the standard deviation between replicates.

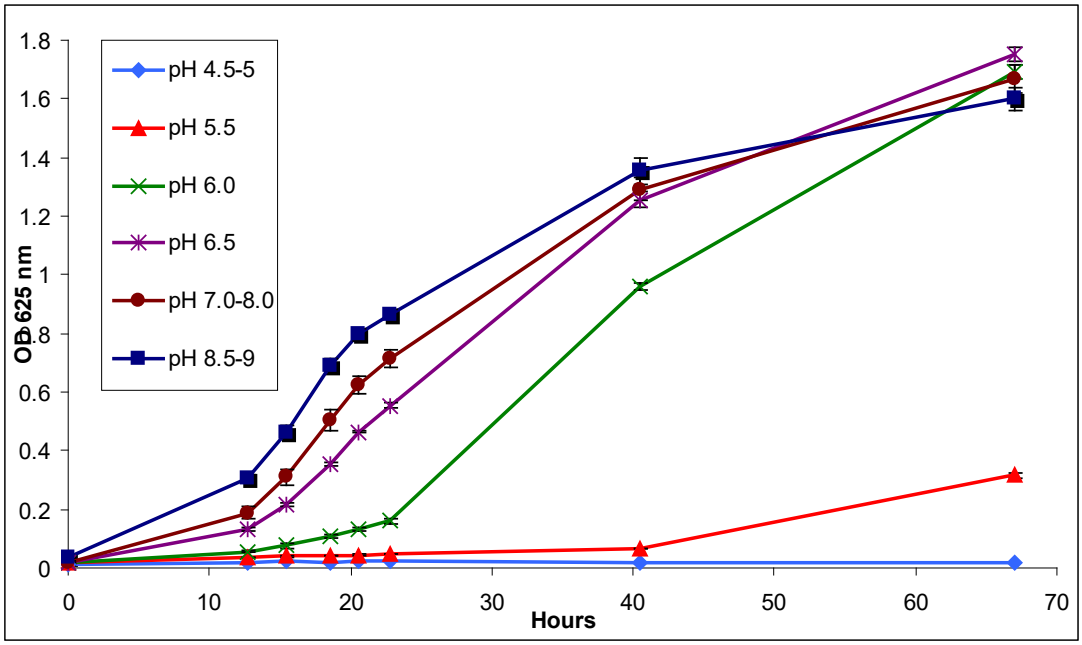

Figure 2.3. Growth of *Bosea* sp. WAO at ten pH values was determined by monitoring the change in OD at 625 nm in trypticase soy broth. The pH values ranged from 4.5- 9 pH and increased by 0.5 pH increments. Data was grouped when similar growth response was obtained. Each point represents a minimum of three replicates per pH concentration with error bars representing the standard deviation between replicates.

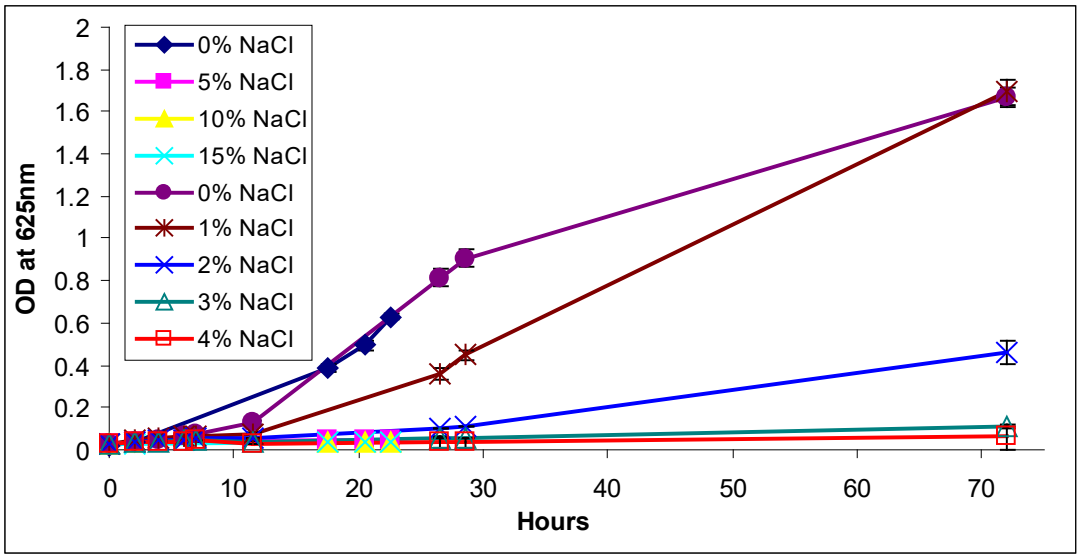

Figure 2.4. Growth of *Bosea* sp. WAO at eight salinities was determined by monitoring the change in OD at 625 nm in trypticase soy broth (0.5 % salinity) with additional NaCl added from 0 % - 15 % weight/volume. Added concentrations 0 % (diamond), 5 %, 10 %, and 15 % were completed with growth only observed in only the control 0 % NaCl. A second round of growth curves with added concentrations between 0 % (circle) through 5 % were completed. Each point represents three replicates with error bars representing the standard deviation between replicates.

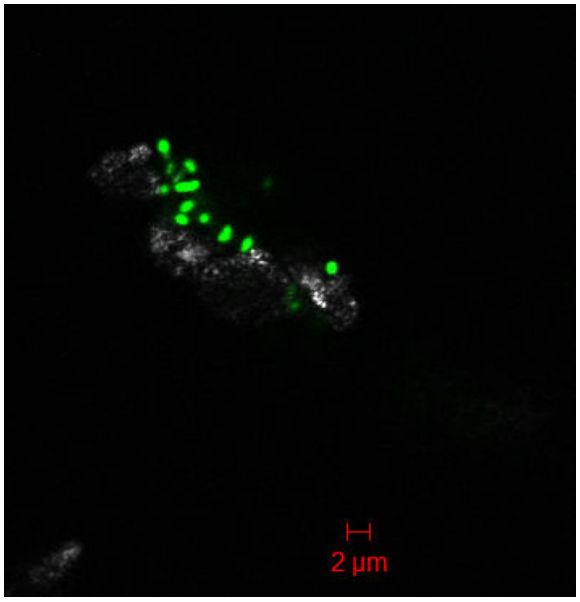

Figure 2.5. Confocal microscopy of *Bosea* sp. WAO. *Bosea* sp. WAO (green) was stained with DAPI and imaged growing on the surface of a small cadmium sulfide particle (white).

Table 2.2. Classification and general features of *Bosea* sp. WAO (Field *et al.*, 2008).

MIGS ID	Property	Term	Evidence code[a]
	Classification	Domain *Bacteria*	TAS (1,2)
		Phylum *Proteobacteria*	TAS (1,2)
		Class *Alphaproteobacteria*	TAS (1,3)
		Order *Rhizobiales*	TAS (1,3)
		Family *Bradyrhizobiaceae*	TAS (1,5)
		Genus *Bosea*	TAS (1,6,7)
		Species sp.	TAS (1)
		Strain: WAO *(DQ986321.1)*	TAS (1)
	Gram stain	Negative	IDA
	Cell shape	Rod	TAS (8)
	Motility	Motile	TAS (8)
	Sporulation	Not reported	NAS
	Temperature range	Mesophile	IDA
	Optimum temperature	25-30 °C	IDA
	pH range; Optimum	6-9; 8	IDA
	Carbon source	D-glucose, lactose, acetate, bicarbonate	TAS (8)
MIGS-6	Habitat	Terrestrial, Black shale	TAS (8)
MIGS-6.3	Salinity	No growth with >3.5 % NaCl (w/v)	IDA
MIGS-22	Oxygen requirement	Aerobic	TAS (8)
MIGS-15	Biotic relationship	free-living	TAS (8)
MIGS-14	Pathogenicity	Not reported	NAS
MIGS-4	Geographic location	Lockatong formation, New Jersey, USA	TAS (8)
MIGS-5	Sample collection	2005	IDA
MIGS-4.1	Latitude	40.289329	IDA
MIGS-4.2	Longitude	-74.814366	IDA
MIGS-4.4	Altitude	60 m	IDA

[a] Evidence codes - IDA: Inferred from Direct Assay; TAS: Traceable Author Statement (i.e., a direct report exists in the literature); NAS: Non-traceable Author Statement (i.e., not directly observed for the living, isolated sample, but based on a generally accepted property for the species, or anecdotal evidence). These evidence codes are from the Gene Ontology project, 2004. (1) Wang *et al.*, 2007. (2) Woese *et al.*, 1990. (3) Garrity *et al.*, 2005b. (4) Kuykendall 2005. (5) Garrity *et al.*, 2005a. (6) Das et al., 1996. (7) Das 2005. (8) Rhine *et al.*, 2008.

Table 2.3. Genome statistics.

Attribute	Value	% of Total
Genome size (bp)	6,125,776	100.00
DNA coding (bp)	5,469,601	89.29
DNA G+C (bp)	4,094,621	66.84
DNA scaffolds	42	100.00
Total genes	5,727	100.00
Protein coding genes	5,665	98.92
RNA genes	62	1.08
Pseudo genes	0	0
Genes in internal clusters		
Genes with function prediction	4740	82.77
Genes assigned to COGs	4193	73.21
Genes with Pfam domains	4837	84.46
Genes with signal peptides	635	11.09
Genes with transmembrane helices	1391	24.29
CRISPR repeats	0	0

Table 2.4. Number of genes associated with general COG functional categories.

Code	Value	%age	Description
J	212	4.44	Translation, ribosomal structure and biogenesis
A	0	0	RNA processing and modification
K	388	8.13	Transcription
L	112	2.35	Replication, recombination and repair
B	3	0.06	Chromatin structure and dynamics
D	29	0.61	Cell cycle control, cell division, chromosome partitioning
V	109	2.28	Defense mechanisms
T	213	4.46	Signal transduction mechanisms
M	239	5.01	Cell wall/membrane biogenesis
N	75	1.57	Cell motility
U	60	1.26	Intracellular trafficking and secretion
O	175	3.66	Posttranslational modification, protein turnover, chaperones
C	333	6.97	Energy production and conversion
G	276	5.78	Carbohydrate transport and metabolism
E	657	13.76	Amino acid transport and metabolism
F	102	2.14	Nucleotide transport and metabolism
H	233	4.88	Coenzyme transport and metabolism
I	249	5.21	Lipid transport and metabolism
P	385	8.06	Inorganic ion transport and metabolism
Q	155	3.25	Secondary metabolites biosynthesis, transport and catabolism
R	470	9.84	General function prediction only
S	268	5.61	Function unknown
-	1534	26.79	Not in COGs

The total is based on the total number of protein coding genes in the genome.

Table 2.5. Comparison of basic genome features of *Bosea* spp.

Genome Name	Status[a]	Genome Size (Mbp)	G+C Content (%)	Gene Count	No. of protein coding genes w/ function prediction	Percentage (%)	No. of protein coding genes in COGs	Percentage (%)	IMG Genome ID
Bosea sp. WAO	D	6.12	67	5727	4570	79.8	4193	73.2	2615840542
Bosea sp. LC85	PD	6.56	65	6267	4975	79.4	4548	72.6	2609460206
Bosea sp. UNC402CLCol	PD	5.61	67	5389	4375	81.1	4067	75.5	2579779168
Bosea lupini DSM 26673	D	6.13	67	5985	4752	79.4	4396	73.4	2634166302
Bosea sp. OK403	D	6.64	65	6099	5066	83.1	4396	77.0	2609459641
Bosea sp. AAP25	PD	4.14	64	3984	3023	75.9	2651	66.5	2636415410
Bosea lathyri DSM 26656	D	5.91	65	5559	4476	80.5	4120	74.1	2622736433
Bosea sp. 117	PD	4.63	68	4344	3639	83.8	3366	77.5	2562617052
Bosea sp. AAP35	PD	4.46	66	4298	3435	79.9	3144	73.1	2636415883
Bosea vaviloviae strain SD260	F	5.60	66	5415	-	-	-	-	N/A
Bosea thiooxidans CGMCC 9174 V5_1	F	5.46	67	5176	-	-	-	-	N/A

These data were obtained from the IMG/ER platform (Markowitz *et al.*, 2012) and NCBI genomes. [a]Status: D=draft, PD=permanent draft, F=finished.

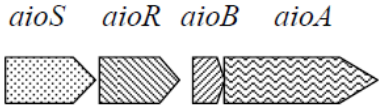

Figure 2.6. Operon Structure for arsenite oxidation viewed 5'-3' direction on the plus strand. The gene order is the same in both *Bosea* sp. WAO and *Bosea* sp. 117 with a senor histidine kinase, *aioS*, then a transcriptional response regulator, *aioR*, followed by the *aioB* and *aioA* genes.

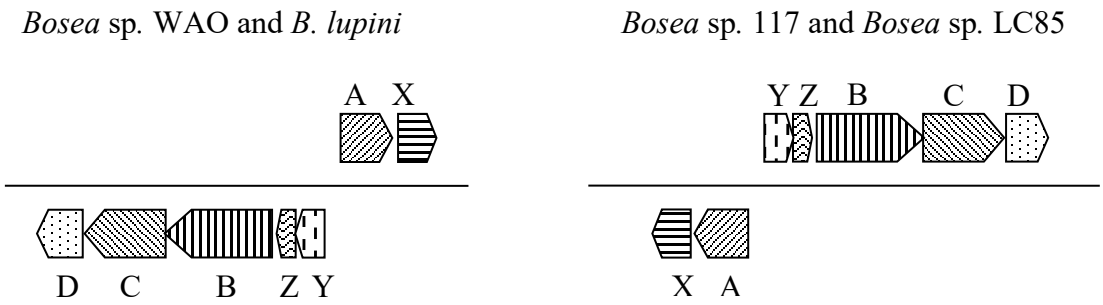

Figure 2.7. Operon structure for the *sox* genes for thiosulfate oxidation. The orientation is 5'-3' with the plus strand on top. The orientation of the genes for *Bosea* sp. WAO and *B. lupini* are the same while *Bosea* sp. LC85 and *Bosea* sp. 117 have the same orientation. These operons are inverted between the plus and minus strands.

Chapter 3:

Transformation of galena to pyromorphite produces bioavailable sulfur for neutrophilic chemoautotrophy

Abstract

The aqueous concentration of lead [Pb] in geochemical environments is controlled by the solubility of Pb-bearing minerals and their weathering products. In contaminated soils, a common method for *in situ* stabilization of Pb is the addition of phosphate to convert more redox sensitive sulfide minerals into sparingly soluble pyromorphite [$Pb_5(PO_4)_3X$]. In this study, I conducted experimental studies to investigate the fate of reduced sulfur during the conversion of galena [PbS] to chloropyromorphite [$Pb_5(PO_4)_3Cl$]. Powder X-ray diffraction analysis indicated that the reaction of phosphate with galena resulted in the formation of elemental sulfur [S_8]. Under abitoic conditions the S_8 was retained in the solid phase, and negligible concentrations of sulfur as sulfide and thiosulfate was detected in the aqueous phase and only a small amount as sulfate. When PbS reacted in the presence of the chemoautotrophic organism *Bosea* sp. WAO, the S_8 in the secondary mineral was oxidized to sulfate. Strain WAO produced significantly more sulfate from the secondary S_8 than from the primary galena. Microscopic analysis of mineral-microbe aggregates on mineral embedded slide cultures showed that the organism was co-localized and increased in biomass over time on the secondary mineral surface supporting a

microbial role. The results of this study indicate that stimulation of sulfur-oxidizing activity may be a direct consequence of phosphate amendments to Pb contaminated soils.

Introduction

With annual world production at approximately 10 megatons, anthropogenic activities have dramatically altered the global geochemical cycle of lead [Pb] and greatly enriched its concentration on the Earth's surface (Holleman and Wiberg 2001b). Mining and refining of galena [PbS] are important sources of Pb contamination to soils and natural waters (Dudka and Adriano 1997). Mineral transformations strongly affect the fate and solubility of Pb during chemical weathering and modification of the mineral conversion process has been used to control the mobility of Pb in contaminated water-rock systems (Ruby *et al.*, 1994, Scheckel *et al.*, 2013). A common method for *in situ* soil stabilization for Pb contamination involves the addition of phosphate to convert more soluble Pb minerals to pyromorphite [$Pb_5(PO_4)_3X$] X=Cl, Br, F, or OH (Ruby *et al.*, 1994, Zhang and Ryan 1999, Martinez *et al.*, 2004, Kumpiene *et al.*, 2008, Scheckel *et al.*, 2013). Secondary pyromorphite-type phases have low Pb solubility and limited bio-accessibility compared to the primary Pb minerals (Kumpiene *et al.*, 2008). Furthermore, pyromorphite is not redox sensitive thus changing the long term Pb stability, particularly in soil environments subject to fluctuating water table levels. A review by Miretzky and Fernandez-Cirelli (2008) extensively covers

phosphate amendments to soils and the effects based on the form of phosphate added as *e.g.* hydroxyapatite, phosphate rock, bone meal, or phosphoric acid. Phosphoric acid was determined to be most effective due to its ease of application and ability to dissolve Pb^{2+} from other minerals enhancing the transformation to pyromorphite (Miretzky and Fernandez-Cirelli 2008). The transformation reaction when both Pb and PO_4 are in solid form is dependent on the dissolution rate of both the Pb mineral and PO_4 mineral (Zhang and Ryan 1999).

Galena [PbS] is a relatively insoluble Pb mineral with a $K_{sp} = 10^{-28.3}$; however, when exposed to oxygen it will spontaneously oxidize the sulfur to sulfate (Hsieh and Huang 1988, Ruby *et al.*, 1994). This can lead to the formation of anglesite ($PbSO_4$) which is more soluble with a $K_{sp} = 10^{-7.7}$ (Ruby et al., 1994, Scheckel 2013). In the absence of complexing agents pH controls the precipitation-dissolution reaction of PbS with dissolved Pb(II) decreasing exponentially with increasing pH (Hsieh and Huang 1988). The addition of phosphate as a complexing agent has been shown to react with the mineral and form pyromorphite which is more stable at ambient oxidizing surface conditions (Zhang and Ryan 1999). The solubility of pyromorphite varies based on pH with acidic conditions pH 0 - 2.12 having a $K_{sp} = 10^{-18.69}$ and basic pH 12.38 – 14 having a $K_{sp} = 10^{-84.4}$, however, when adjusted for normal soil range of pH 3 - 7 the $K_{sp} = 10^{-25.05}$ is more realistic (Scheckel *et al.*, 2013). This transformation reaction in the environment occurs primarily by the dissolution of hydroxyapatite

[$Ca_5(PO_4)_3OH$] and the precipitation of hydroxypyromorphite [$Pb_{10}(PO_4)_6OH_2$] (Ruby *et al.*, 1994, Martinez *et al.*, 2004). The conversion of galena to pyromorphite is effective for immobilizing the Pb but the fate of the reduced sulfur from the primary sulfide mineral is poorly understood in comparison to dissolution of pure PbS.

The dissolution of PbS has been studied in dilute aqueous solutions in the absence of phosphate by varying pH, electrochemical potentials, and in the presence and absence of oxygen (Hsieh and Huang 1989, De Giudici and Zuddas 2001, De Giudici *et al.*, 2004, Hampton *et al.*, 2010). Early studies looked at overall solution chemistry while more recent work has focused on atomic force microscopy to view mineral surface changes, using electrochemistry as their oxidant. Using bulk solution chemistry dissolution of 2 mM $PbS_{(s)}$ over six hours showed a maximum of 60 μM Pb(II) in solution at pH 2.5 and dissolution deceased exponentially as pH increased from pH 2.5 to 9 with limited dissolution above pH 8 (Hsieh and Huang 1988). They determined that in the absence of oxygen, PbS dissolution occurs from the protonated surface with the release of Pb(II) and H_2S into the bulk phase (Hsieh and Huang 1988). Whereas in the presence of oxygen, the oxygen molecule is absorbed onto the protonated PbS surface and releases as sulfate and Pb(II). Whereas when AFM techniques and solution chemistry were combined, Giudici and Zuddas (2001), observed an initial surface pitting followed by the formation of protrusions from the PbS surface. They predicted based on literature data that these protrusions were composed of

native sulfur that were less soluble and were slowly being oxidized to sulfate (Giudici and Zuddas 2001). As the dissolution reaction progresses a surface coating forms of these protrusions causing the reaction to slow down and become kinetically inhibited (De Giudici and Zuddas 2001). Hampton *et al*. (2011) used electrochemistry to show that they could oxidize PbS to form elemental sulfur and Pb^{2+} under deoxygenated conditions. When the electrochemically oxidized surfaces were examined with AFM they observed deposits that were confirmed with Raman spectroscopy to be elemental sulfur (Hampton *et al*., 2011). Under conditions without phosphate: hydrogen sulfide, elemental sulfur, and sulfate have been observed as products of the dissolution reaction. Although the studies do not agree on the oxidation state of the sulfur released they all indicate that reduced sulfur is present after PbS begins to dissolve.

The fate of sulfur from the transformation of galena to pyromorphite has been largely ignored, as few studies focus solely on one mineral form of Pb and are instead studying the bulk mobility of the Pb^{2+} and not the associated mineral components. Zhang and Ryan (1999) examined the release of both Pb and S with a phosphate amendment of hydroxyapatite [$Ca_5(PO_4)_3OH$] under abiotic conditions and were able to detect a maximum of 8 % S after formation of chloropyromorphite. They determined that only 9 % of the galena was transformed and that the reaction was inhibited by the slow oxidation of sulfide (Zhang and Ryan 1999). The nucleation and growth of pyromorphite particles on

galena was observed using electrochemical scanning tunneling microscopy and determined that the particles grow epitaxially (Stack *et al.*, 2004). This study also proposed that phosphate passivates the PbS surface either by inhibiting the retreat of steps or by stabilizing lead-terminated surface structure and thereby inhibiting further dissolutions (Stack *et al.*, 2004). A site study looking at a port facility where concentrated galena ore and dross was stored and transported in close proximity to a phosphoric acid plant, determined that the galena was being weathered to lead phosphates (Ruby *et al.*, 1994).

Previous studies examining microbial activity in relation to soil amendments have focused on utilizing microbes for enhancing the solubility of the phosphate amendments and consequently increasing the reaction of phosphate with Pb (Wilson *et al.*, 2006, Park *et al.*, 2011, Park and Bolan 2013). Bacteria have been shown to release organic acids that decrease the pH and increase the solubility of rock phosphate (Park *et al.*, 2011). These phosphate solubilizing bacteria (PSB) enhance the reaction of insoluble phosphates with Pb in soil and agar medium (Park and Bolan 2013). The combination of different organisms with three types of phosphate amendments caused a decrease in Pb availability (Wilson *et al.*, 2006). To date, very little is known about how microorganisms might be able to use the reduced sulfur produced during phosphate amendments for chemoautotrophic growth. Since S is a well-known electron donor for microbial growth, I hypothesize that the reaction of phosphate

with PbS in oxic conditions results in the formation of bioavailable sulfur for chemoautotrophic growth.

In this study, I conducted experiments to investigate the bio-oxidation of reduced sulfur in PbS and how phosphate amendments stimulate the activity of neutrophilic sulfide oxidizing bacteria (SOB). The objective of this work was to determine the partitioning and bioavailability of sulfur from galena after reaction with phosphate. The results of this study provide new insights into the complex biogeochemical processes that occur during sulfide mineral transformations.

Materials and Methods

Bacterial Strain. I used the microorganism *Bosea* sp. WAO a facultative chemolithoautotroph previously isolated from black shale obtained from the Lockatong geological formation in the Newark Basin near Trenton, New Jersey (Rhine *et al*., 2008). Strain WAO is a neutrophilic chemolithoautotroph that was first isolated on CO_2 and arsenite [As(III)], that is oxidized to arsenate [As(V)] (Rhine *et al*., 2008). From the mineral arsenopyrite [AsFeS], this organism oxidized and released stoichiometric amounts of As(III) to As(V), S^{2-} to SO_4^{2-}, and Fe(II) to Fe(III) bound in arsenopyrite (Rhine *et al*., 2008).

Mineral Synthesis and Characterization. Lead sulfide was synthesized by mixing sterile anaerobic stocks of Na_2S and $Pb(II)(NO_2)_3$ (Simpson *et al*., 1998). After precipitation the mineral was triple washed with degassed water by exchanging volumes but not filtering. The stock mineral was characterized using

X-ray diffraction (XRD) spectroscopy to confirm successful synthesis of the desired mineral.

Powder X-ray Diffraction Analysis. The XRD analyses were conducted by a Bruker D8 Discover instrument, equipped with an IμS Cu microsource of 1.54 Angstrom wavelength which provided an X-ray beam through a 2 mm point collimator. The X-ray diffraction pattern was detected by a Vantec 500 2D detector. The X-ray source's operating conditions were voltage of 50 kV, and current of 1000 μA.

All samples were pipetted from solution onto a glass plate and were subjected to N_2 atmosphere. Nitrogen stream assisted in quicker evaporation of the solvent and drying out of the sample for analysis, as well as in eliminating possible oxidation reactions with atmospheric oxygen during the process of evaporation. The glass slide was stabilized on a CLC rotating stage.

The phosphate reacted samples +/- strain WAO were analyzed by conducting scans of 10-steps from 10 to 50 2theta, with 5000 seconds per step (14 hours run). The galena stock sample was analyzed with a 7-step scan, ranging from 5 to 65 2theta and 120 seconds per step (14 minutes run).

Chemical Analysis of S. Voltammetric analyses were conducted on several experimental solutions to determine the presence of electrochemically active sulfur species, including H_2S/HS^-, S_n^{2-}, S_8, $S_2O_3^{2-}$, $S_4O_6^{2-}$, and HSO_3^{2-} (Luther III *et al.*, 2001, Druschel *et al.*, 2004, Boyd and Druschel, 2013). Detection limits for sulfide and polysulfide are very low, 0.2 μmol/dm^{-3} whereas detection limits for

thiosulfate and polythionates are much higher, 15-16 μmol/dm^{-3} (Luther *et al.*, 2001). Detection limits for elemental sulfur are also low, but not all forms of elemental sulfur are electroactive and detectable at all using voltammetric analyses (Boyd and Druschel, 2013). Voltammetric analyses were carried out with an Analytical Instrument Systems, Inc., DLK-60 potentiostat and computer controller. The voltammetric system consists of three electrodes: a silver/silver chloride reference electrode, a platinum counter electrode, and an Au-amalgam working electrode (after Brendel and Luther, 1995; Luther *et al.*, 2008). Experimental solutions were placed in a 30 mL reaction cell that was purged with N_2 for 4 min to remove dissolved molecular oxygen. Cyclic voltammetry scans between -0.1 and -1.8 V v. Ag/AgCl were conducted at a scan rate of 1000 mV/sec with or without a 2-s conditioning step. Conditioning steps were utilized for low sulfide concentrations to provide lower detection limits for sulfide (nM levels; Luther *et al.*, 2008). Calibrations were carried out directly by standard addition of analytes of interest in matrix-matched solutions. Thiosulfate and sulfate were analyzed by Ion Chromatograhy on a Dionex ICS-1100 using an AS14 analytical column and AG-14 guard column. Polysulfide was analyzed after derivatization of by methyl triflate on a Thermo Scientific Ultimate3000 HPLC using a C18 column for separation and single channel UV detector at 400nM (after Kamyshny *et al.*, 2004, Kamyshny *et al.*, 2006).

Medium. A mineral salts medium was used for all experimental growth conditions that was absent of soluble sulfur sources. One liter of medium

contained 0.3 g NH_4Cl, 0.1 g $MgCl_4$ + 7 H_2O, 5 mL VS mineral solution, 1 mL S8 vitamin solution, plus 10 mM bicarbonate. The VS minerals for a 200 mL stock were 10 g EDTA, 2.09 g $ZnCl_2$ + H_2O, 1.73 g $CaCl_2$ + $2H_2O$, 1.6 g $MnCl_2$ + $4H_2O$, 0.72 g $FeCl_2$ + 4 H2O, 0.22 g $(NH_4)_2Mo_7O_{24}$ + 4 H_20, 0.22 g $CuCl_2$ + $2H_2O$, 0.32 g $CoCl_2$ + $6H_2O$. The S8 vitamin stock for a one Liter stock is 2 mg Biotin, 2 mg folic acid, 10 mg pyridoxine HCl, 5 mg Riboflavin, 5 mg nicotinic acid, 5 mg pantothenic acid, 0.1 mg vitamin B12, 0.005 mg P-amino benzoic acid, and 0.005 mg thiocetic acid. Experiments were run with or without the addition of 7.9 g Na_2HPO_4 + $7H_2O$ and 1.5 g KH_2PO_4.

Culture Conditions. To examine the effect of phosphate on mineral sulfide oxidation, the production of sulfate from PbS was monitored over time. Experiments were conducted to compare the rate and extent of oxidation with and without the addition of phosphate. Three sets of conditions: sterile control, abiotic control, and active cultures were established with 40 mM phosphate and two sets of conditions: abiotic control and active cultures without phosphate. Sterile controls in duplicate contained minimal medium, strain WAO autoclaved three times, and 2 mM PbS to determine if dead cellular material affected oxidation. Background controls in duplicate consisted of only medium, amended with 2 mM PbS to account for any abiotic transformations that might occur. Active cultures in triplicate contained medium, strain WAO, and 2 mM PbS. Cultures were incubated in the dark at 30 °C on an orbital shaker to provide aeration.

At each time point samples were taken from all conditions and all replicates to analyze for sulfate and phosphate concentrations. An aliquot of 0.8 mL was removed and immediately filtered through a Spin-X filter tube and frozen until analysis to prevent further oxidation of compounds. Dissolved sulfate and phosphate concentrations were determined using ion chromatography on a Dionex® DX-120 with a Dionex Amms 300 suppressor. The guard column was a RFIC IonPac® AG14A 4 x 50 mm and the analytical column was an RFIC IonPac® AS14A 4x 250 mm.

Mineral Embedded Slide Cultures for Microscopy. Slide cultures were prepared to visualize cell growth on a particle surface without the use of filtering. Sterile slides were coated with a thin layer of hot noble ager and dusted with PbS powder. Once cooled, the excess PbS powder was tapped off of the slide leaving only the adhered mineral. Replicate slides were placed into individual sterile Petri plates with minimal salts medium containing 40 mM phosphate. Sterile media was added until the slide surface was submerged creating a growth chamber. Strain WAO was then added to each growth chamber to allow for colonization on the mineral particles embedded on the slide. The replicate growth chambers were incubated for 1, 4, or 6 days at 30 ºC in the dark. The slides sacrificed at each time point were transferred to a sterile bath of 4 % gluteraldehyde in phosphate buffer to fix cells for 15 minutes. The slide was then removed and placed into a series of MilliQ water baths to gently wash away any excess gluteraldehyde. Slides were transferred to a sterile bath containing 0.1 mg/mL

ethidium bromide or 25 µg/mL DAPI for 15 minutes to stain. Another set of MilliQ water baths were used to remove excess ethidium bromide or DAPI stain. After the last water bath a coverslip was placed onto the slide and sealed on all sides with clear nail polish.

The slides were examined with either fluorescence or confocal microscopy. Confocal microscopy images were obtained with a Zeiss LSM510 Meta Confocal Laser Scanning Microscope at 630X with water immersion. The secondary mineral image was obtained by collecting the reflection of the 488 nm argon laser source from the mineral surface while the cells were imaged by exciting DAPI with a 364 nm laser source. Fluorescence microscopy images were obtained using a Ziess Axioscope microscope using a mercury lamp. Biomass was viewed at 400x using the Ziess DAPI/FITC/Texas Red filter set to observe the ethidium bromide fluorescence.

Results

The reaction of galena [PbS] with phosphate resulted in the formation of chloropyromorphite [$Pb_5(PO_4)_3Cl$] and elemental sulfur [S_8]. X-ray diffraction analysis of the primary galena and secondary mineral products formed by the phosphate reaction indicated that mineral transformation had occurred (Fig. 3.1). After reaction with phosphate, the X-ray diffraction pattern showed the loss of the characteristic galena peaks at 2theta = 26, 44, 51, and 54. No residual galena was detected indicating the original material was completely dissolved.

The diffraction pattern of the reacted mineral exhibited peaks that match the reference peaks for chloropyromorphite at 2theta = 21, 22, 27, 28, and 32. Notably, a peak at 2theta = 23 was observed which indicated the formation of an additional secondary mineral product other than pyromorphite. This peak corresponds to the strongest peak in the S_8 reference pattern suggesting that solid-phase reduced sulfur was also formed in the reaction.

The conversion of galena to chloropyromorphite under abiotic conditions released small amounts of reduced sulfur into the aqueous phase. Chemical analysis of the sulfur species was conducted on the abiotic galena transformation samples to determine speciation of sulfur when *Bosea* sp. WAO was absent. Sulfide concentration was measured using cyclic voltammetry which determined that the reaction of 2 mM PbS with phosphate produced no detectable aqueous sulfide. Thiosulfate, sulfide, and polysulfide concentrations were below detection limits. In the absence of phosphate, sulfate accounted for 12 % of the sulfur species after 20 days in the abitoic control (Fig. 3.2a); however, with phosphate addition sulfate accounted for only 3.5 % of sulfur species after 18 days of reaction (Fig. 3.2b). The data indicate that limited sulfur from the PbS mineral is being abiotically oxidized and released into the aqueous phase during its transformation with phosphate to chloropyromorphite. Finally, to test if sulfide was released from galena and re-absorbed onto the secondary pyromorphite surfaces, I conducted an excess sulfide sorption experiment using cyclic voltammetry. After the secondary mineral product was formed aliquots of sulfide

were added into the reaction vessel. The results showed that sulfide did not sorb to the mineral surface (data not shown). Together, the data indicate that during the conversion of galena to chloropyromorphite under abiotic conditions, sulfur is being retained in the solid phase.

I examined if the elemental sulfur formed during the conversion of galena to chloropyromorphite is consumed by the chemoautotrophic microorganism, *Bosea* sp. WAO. When galena reacts with phosphate in the presence of strain WAO, the diffraction peak at 2theta = 23 is absent in the X-ray diffractogram, indicating that elemental sulfur does not accumulate in the presence of bacterial cells. The reaction of galena with phosphate in the presence of bacterial cells does not inhibit the precipitation of pyromorphite as the X-ray diffraction peaks associated with pyromorphite are identical in both conditions. However, the loss of X-ray diffraction peak at 2theta = 23 suggests that the elemental sulfur is a bioavailable form of sulfur for microbial oxidation.

The reaction of phosphate with galena increased the bioavailability of sulfur for chemoautotrophic metabolism (Fig. 3.2). Strain WAO produced 50 % more sulfate from the secondary mineral than from the primary galena (Fig. 3.2). When the primary mineral was incubated with strain WAO, a maximum of 38 % of sulfur was oxidized to sulfate in twenty days (Fig. 3.2a). In comparison, over 90 % of the sulfur was oxidized to sulfate when the galena reacted with phosphate (Fig. 3.2b). Abiotic control experiments for both minerals showed small amounts of sulfate formation in the absence of cells: 12 % for the primary

mineral and 3.5 % when transformed with phosphate (Fig. 3.2). Sulfate concentration in the sterile controls matched the sulfate concentration observed in the abiotic controls for the secondary mineral oxidation experiment (data not shown).

Sulfur oxidation of the secondary mineral products is concurrent with bacterial growth (Fig. 3.3). Confocal and fluorescent microscopy revealed that strain WAO colonized the mineral surface, and that the biomass increased over time (Fig. 3.3). Colonization was studied using slide cultures imaged with confocal and fluorescent microscopy. Confocal images of a single focal plane show the cells are co-localized with the mineral particles, indicating that the cells and secondary mineral products are in close association (Fig. 3.3a). The multi-stack rendering show cells are only present on the mineral surface and not observed away from the particle, indicating that the cells are colonizing the mineral surface (Fig. 3.3b). Fluorescent microscopy images of replicate slides showed increasing colonization of the mineral surface with longer incubation, indicating cells are growing in association with the solid phase (Fig. 3.3c). Reduced sulfur as a solid is the only electron donor in this system, and no organic carbon is present, suggesting growth of strain WAO requires contact with the mineral surface.

Discussion

I can describe the transformation of galena to chloropyromorphite with the following reaction:

$$5PbS_{(s)} + 3HPO_4^{2-}{}_{(aq)} + Cl^-_{(aq)} + 5O_{2(aq)} + 7H^+_{(aq)} \rightarrow Pb_5(PO_4)_3Cl_{(s)} + 5S_{(s)} + 5H_2O_{(l)} \quad (1)$$

$\Delta G_r° = -1084.74$ kJ/mol

The formation of chloropyromorphite by the reaction of galena with phosphate is in agreement with previous studies (Ruby *et al.*, 1994, Zhang and Ryan 1999, Martinez *et al.*, 2004, Kumpiene *et al.* 2008, Scheckel *et al.*, 2013). This reaction is exothermic and has a Gibbs Free Energy of reaction when calculated at standard conditions of $\Delta G_r° = -1084.74$ kJ/mol. However, under the conditions in my experiments (T= 30 °C, $[O_2] = 0.234$ mM, $[PO_4^{2-}] = 40$ mM, $[Cl^-] = 7.86$ mM, and pH = 7.3) the Gibbs free energy of reaction showed a decrease for equation 1 to $\Delta G_r = -646.29$ kJ/mol (supplemental data, appendix). Thermodynamic calculations indicate this mineral transformation reaction is energetically favorable in oxic neutral pH waters containing phosphate and chloride (supplemental data, appendix). In my experiments, I worked with high phosphate levels in order to observe a rapid conversion and maximize the extent of transformation. The ideal molar ratio based on the pyromorphite structure is a ratio of Pb:P of 5:3 or 1.667. Although galena is thermodynamically unstable at this Pb:P ratio, phosphate concentrations in the environment must be much higher to overcome other side reactions (Scheckel *et al.*, 2013). Here my use of

soluble phosphate and ratio of Pb:P = 1:20 was employed to favor complete conversion of the galena and to facilitate the detection of side products of the reaction.

Of significance in my study was the detection of elemental sulfur as a secondary mineral product, which to my knowledge had not been reported without the use of electrochemical oxidation (Stack *et al.*, 2004). The experimental data demonstrated that the S_8 in the solid phase produced from the transformation of galena to pyromorphite is a significant pool of reduced sulfur available for chemoautotrophic growth. In the absence of cells, only 3.5 % of the reduced sulfur was measured in the aqueous phase (Fig. 3.2b) indicating that elemental sulfur accumulated in solid form as the primary S-containing transformation product. In contrast, the galena transformation experiments conducted with strain WAO did not show the accumulation of elemental sulfur, suggesting that the microbes are metabolizing S_8. Strain WAO is able to grow chemolithoautotrophically by oxidizing several sulfur species to sulfate, including sulfide, polysulfide, sulfur and thiosulfate (Rhine *et al.*, 2008). In addition to dissolving the PbS and precipitating chloropyromorphite, the phosphate reaction is changing the bioavailability of reduced sulfur originally bound in PbS. In the control experiment with pure galena strain WAO was able to rapidly oxidize a maximum of 37.5 % of the 2 mM sulfur from the PbS mineral (Fig. 3.2a). In the mineral transformation experiment with phosphate these same organisms are able to access and oxidize 90 % of the elemental sulfur to sulfate (Fig. 3.2b).

The phosphate addition increased the sulfur bioavailability allowing the microorganisms to more easily access the sulfur and oxidize it to obtain energy for chemolithoautotrophic growth. Therefore, the phosphate amendments for attenuating Pb from PbS in soils may stimulate the sulfur oxidizing population of the microbial community and increase the amount of sulfate released into the surrounding environment.

I can describe aerobic microbial oxidation of elemental sulfur with the following reaction:

$$S_{(s)} + 1.5O_{2(aq)} + H_2O \rightarrow SO_4^{2-} + 2H^+ \qquad (2)$$

$$\Delta G_r^\circ = -507.42 \text{ kJ/mol}$$

Under standard conditions equation 2 is also exothermic with a Gibbs Free Energy of reaction of $\Delta G_r^\circ = -507.42$ kJ/mol. When determined with my experimental conditions (T= 30 °C, $[O_2] = 0.236$ mM, $[SO_4^{2-}] = 2$ µM and pH = 7.3) the Gibbs free energy of equation 2 is more energy yielding at $\Delta G_r = -593.67$ kJ/mol. This reaction is energetically favorable at more basic pH values, high oxygen concentration and low sulfate concentration (see supplemental data, appendix). Because the abiotic oxidation of elemental sulfur is often kinetically inhibited, chemolithoautrophic organisms such as strain WAO can take advantage of the redox disequilibrium and harness energy from this reaction. Indeed, the ability of strain WAO to oxidize secondary elemental sulfur highlights the importance of neutrophilic chemoautotrophy in contaminated environmental systems. Microorganisms are known to oxidize sulfide minerals such as pyrite

[FeS_2] in mine tailings, but in those situations both the iron and the sulfide undergo oxidation at acidic pH conditions (Nordstrom and Southam 1997). In my experiments, the addition of phosphate buffers the system and allows neutrophilic microorganisms such as strain WAO to flourish. Strain WAO is a neutral oxidizer that thrives between pH 6-10, optimally growing at pH 8. This is in contrast to many other mineral sulfide oxidizers that require acidic conditions for their metabolic activity (Norris *et al.*, 1996, Okibe *et al.*, 2003, Rohwerder *et al.*, 2007, Ehrlich and Newman 2008a). Here I begin with a sulfide mineral that is abiotically oxidized to elemental sulfur, this sulfur is now available to the numerous chemolithoautrophic organisms that use sulfur oxidization to obtain energy for carbon dioxide fixation (Kelly 1999, Robertson and Kuenen 2006, Kelly and Wood 2013).

The close association of strain WAO and the secondary mineral products were imaged using confocal microscopy (Fig. 3.3a&b). By embedding the mineral on a slide surface the culture did not have to be filtered onto a membrane for microscopy and potentially cause a false positive association. Images of the mineral particle surface indicated that the organism was co-localized with the surface of the particles (Fig. 3.3 a&b) and the time-course images showed an increase in biomass over time indicating the organisms are growing on the surface of the pyromorphite (Fig. 3.3c). These results suggest that the microorganisms maintain contact with their energy source and increase in biomass on the surface. Since previous experiments indicated that the elemental

sulfur is retained in the solid phase the cells are preferentially colonizing the surface to have access to the bioavailable mineral associated elemental sulfur.

The results of this study indicate that stimulation of sulfur oxidizing activity may be a direct consequence of phosphate amendments to Pb contaminated soils. My findings build on the growing understanding of complex interactions between microorganisms and the Pb-bearing phases in contaminated soils, including the ability of microorganisms to increase the solubility of the different types of phosphate additions such as phosphate rock and microorganisms that are able to produce surface active compounds that would bind metals (Wilson *et al.*, 2006, Park *et al.*, 2011, Park and Bolan 2013). In addition to direct action by microbes on minerals in the environment, these subtler indirect actions as demonstrated here, underscore the complex role that microbes can play in mineral conversions during geochemical processes. Furthermore, understanding these complex interactions allows for improved modeling of both the geochemical and biological aspects of lead sulfide mineral transformation in contaminated sites.

Figures

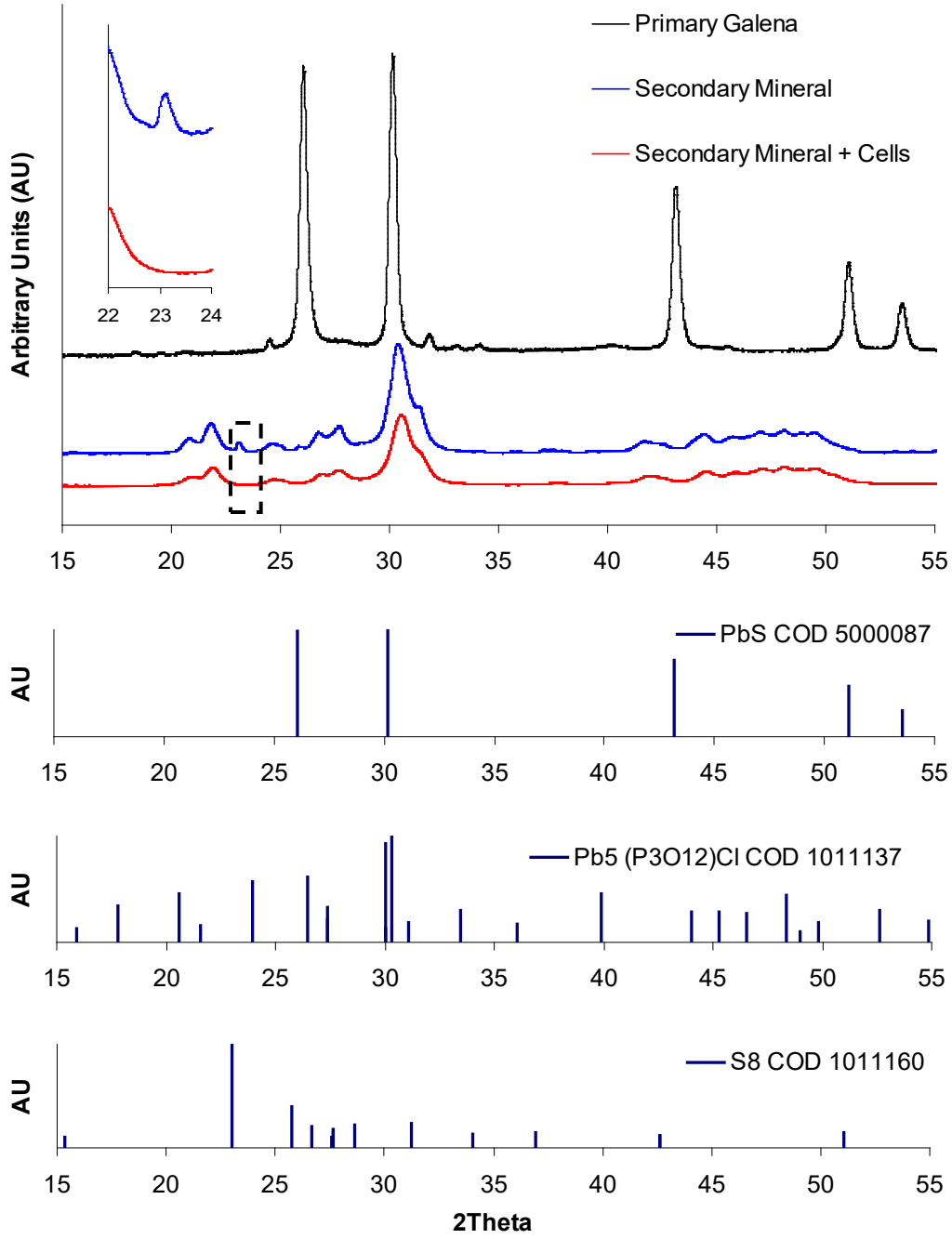

Figure 3.1. X-ray diffraction pattern of minerals before and after reaction with phosphate. Primary Galena [PbS] (black), secondary mineral (blue), and secondary mineral with *Bosea* sp. WAO (red). The inset expands region around the peak at 2theta = 23° to highlight the difference between secondary mineral patterns. The peak at 2theta = 23° is absent in the microbial reacted mineral. Below are the reference peaks for galena [PbS], pyromorphite [$Pb_5(PO_4)_3Cl$] and sulfur [S_8].

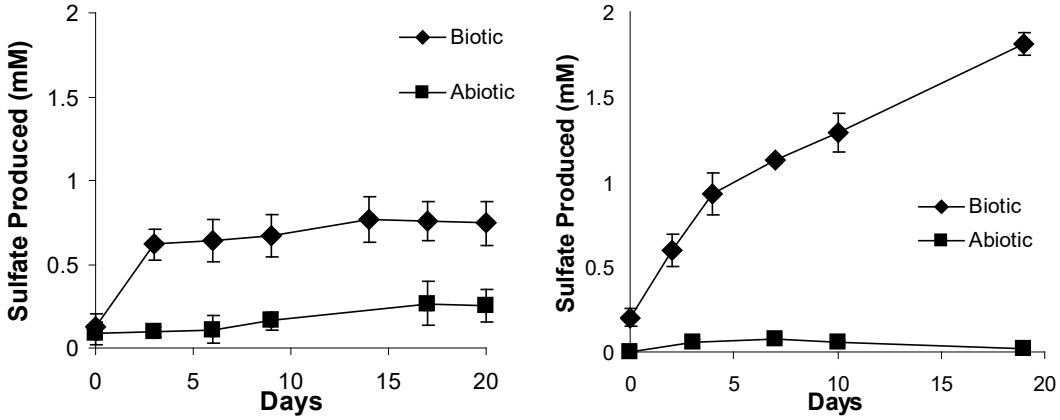

a. No Phosphate Addition b. 40 mM Phosphate Addition

Figure 3.2. Effect of Phosphate on Sulfate Production. Sulfate produced from primary mineral galena vs secondary mineral in the presence (Biotic) and absence (Abiotic) of *Bosea* sp. WAO. a) 2 mM primary galena experiment had 5 replicates of + WAO and 3 replicates -WAO. b) 2 mM secondary mineral (pyromorphite [$Pb_5(PO_4)_3$] and sulfur [S_8]) experiment had 3 replicates of +WAO and 2 replicates –WAO. Sulfate was measured using ion chromatography.

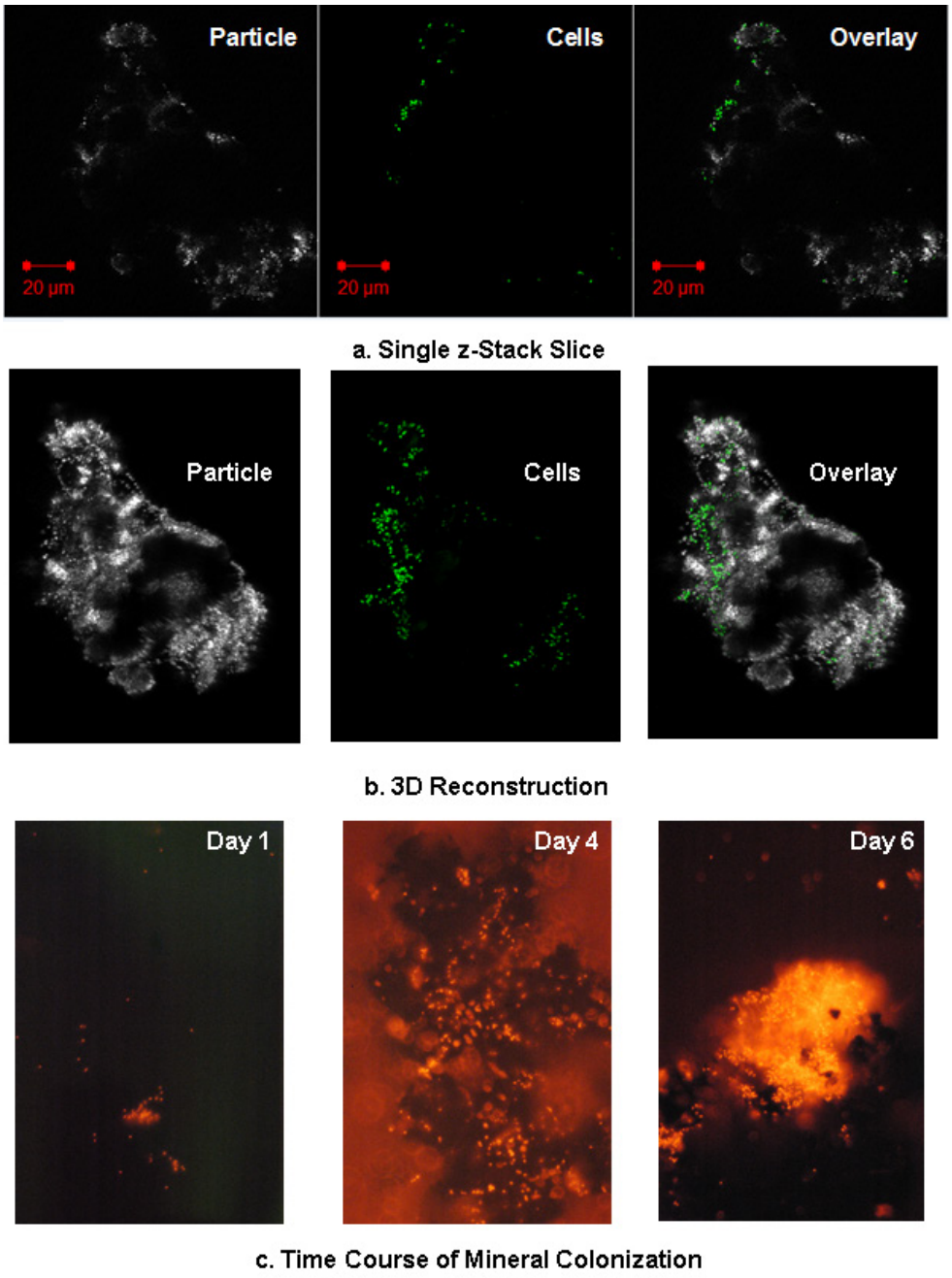

Figure 3.3. Colonization of phosphate reacted mineral particle surface by strain WAO. The slide culture inoculation and stain procedure was used to observe cells without the need for filtration, which would potentially produce an artificial association of the microorganism with the particle surface. a) Single 0.5 µm sample plane of confocal microscopy panels from left to right particle (white), cells (green), and overlay of both. b) 3D rendering of 30 0.5 µm z-stack slices panel from left to right particle (white), cells (green), and overlay of both. The cells are colocalized with the white secondary mineral surface. c) Images obtained from fluorescent microscopy, cells (orange) and the mineral unstained (black), of replicate slide cultures sacrificed after 1, 4, or 6 days of incubation from left to right.

Chapter 4:

Insolubility of Antimony Compounds at Neutral pH has limited the Widespread Development of Microorganisms Capable of Growth on Antimony

Abstract

The concentration of antimony in sediment pore water is limited by the solubility of its compounds. Most naturally occurring antimony compounds are highly insoluble at neutral pH and require acids to increase solubility. Four microorganisms, *Bosea* sp. WAO, *Starkeya novella*, *Thiomicrospira crunogena* EPR75 and *Halothiobacillus hydrothermailis* EPR 155, unable to utilize sodium tartrate as a carbon source, were used to study growth on the electron donors potassium antimony tartrate and elemental antimony. The organisms did not grow on either elemental or potassium antimonyl tartrate. When *Bosea* sp. WAO was given stibnite (Sb_2S_3), the most common form of antimony in the environment, as an electron donor it was able to oxidize the sulfur source to sulfate at an initial rate of 0.32 mM SO_4^{2-}/day compared to background and sterile controls at less than 0.037 mM SO_4^{2-}/day. However, complete oxidation of the sulfide to sulfate was not observed and total concentrations of soluble sulfate at the end of the time course were similar between all conditions suggesting that additional reactions are taking place. Studies that tease apart the sulfur oxidation

and antimony oxidation by using antimony trioxide will help to elucidate if the oxidation is actually due to microbial activity.

Introduction

Antimony is a rare earth element that is naturally occurring and belongs to group 15 of the Periodic Table of Elements below arsenic. It has four possible oxidation states -3, 0, +3, and +5. In the environment it has an average concentration of in 0.2 ppm in igneous rock, 1.5 ppm in shales, 0.3 ppm in limestone, 0.05 ppm in sandstone, 1 ppm in soil, 0.124 ppb in seawater, and 0.2 ppb in freshwater (Ehrlich and Newman 2008b, Filella *et al.*, 2002). Antimony mainly occurs as stibnite (Sb_2S_3), and valentinite (Sb_2O_3) an oxidation product of stibnite (Filella *et al.*, 2002). In industry metallic antimony ore is obtained from stibnite (Holleman and Wiberg 2001a). Elemental antimony is not soluble in non-oxidizing acids but is soluble in nitric acid, while stibnite is soluble in strong acids. At neutral pH neither of these compounds are soluble. However, antinomy trioxide dissolves in tartaric acid to produce potassium antimonyl tartrate which is soluble (Holleman and Wiberg 2001a).

Due to anthropogenic activities, antimony at the surface has been enriched by an order of 70 times (Filella *et al.*, 2002). Antimony has historically been used in cosmetics and is now used in semiconductors, in alloys of lead and tin, in therapeutic agents for tropical diseases and increasingly in flame retardants (Holleman and Wiberg 2001a, Filella *et al.*, 2002). The increased

utilization in flame retardants has reduced the amount of antimony that is recoverable and reused, increasing the potential for environmental contamination (Filella *et al.*, 2002). Stibnite is used in the production of matches, munitions, fireworks, ruby glass, and dyes for plastics (Holleman and Wiberg 2001a). The U.S. EPA considers antimony a pollutant of priority interest and has set a maximum contaminant limit in drinking water of 6 µg/L (Filella *et al.*, 2002).

Studies of microbial interactions with antimony have focused on mining areas with low pH or used the soluble form potassium antimonyl tartrate. Torma and Gabra (1977) show that *Thiobacillus ferrooxidans* (now *Acidothiobacillus ferrooxidans*) was able to optimally oxidize the sulfur in stibnite to sulfate at pH 1.75 and 35 °C. They also showed that 5-7 % of the antimony was oxidized from Sb(III) to Sb(V) but could not confirm if the antimony oxidation was due to direct microbial activity (Torma and Gabra 1977). Studies of other organisms isolated on antimony sulfide ore in acidic environments have shown that the organisms grow and oxidize the sulfur but the fate of the antimony is unclear (Tsaplina *et al.*, 2010, Zhuravleva *et al.*, 2011). Additionally, microbes have been shown to have resistance to antimony by removing Sb(III) using efflux pumps such as the ArsB protein, Acr3p family, and the ABC (ATP-binding cassette) transporter (Filella *et al.*, 2007). Both ArsB and Acr3p have previously been shown to be involved in arsenic resistance (Filella *et al.*, 2007). Studies using the soluble potassium antimonyl tartrate have shown that Sb(III) resistant bacteria are

capable of oxidizing the Sb(III) to Sb(V) and that growth was observed during this activity (Lehr *et al.*, 2007, Li *et al.*, 2013).

In this study I looked at the ability of four neutrophilic microorganisms to grow on several antimony compounds. Most previous studies were conducted at low pH to increase the solubility of Sb compounds or utilized potassium antimony (III) tartrate to study oxidation as it is one of the few soluble forms. The use of the tartrate ligand (HOOC-CHOH-CHOH-COOH) complicates growth studies as this introduces an organic carbon source into the experiment. Here I determined if my organisms of interest could grow on potassium tartrate alone. These organisms were selected because they are capable of both heterotrophic growth and chemolithoautotrophic growth using thiosulfate. I believe that the microorganisms will be unable to grow using antimony compounds as an electron donor as the low solubility of the compounds in the environment would not have favored the development of enzymes necessary for utilization, instead any oxidation is linked to detoxification.

Materials and Methods

Bacterial Strains. The microorganism *Bosea* sp. WAO is a facultative chemoautotroph previously isolated from black shale containing arsenic (Rhine *et al.*, 2008). This organism is a neutrophilic chemolithoautotroph that was first isolated on CO_2 and arsenite, As(III), that is oxidized to arsenate, As(V) (Rhine *et al.*, 2008). Additionally this organism mediates the oxidation of As(III) to

As(V), S^{2-} to SO_4^{2-}, and Fe(II) to Fe(III) bound in arsenopyrite (AsFeS) (Rhine *et al*,. 2008).

The microorganism *Starkeya novella* was isolated by Starkey (1934) and described as the first facultative heterotroph able to grow chemoautotrophically with thiosulfate as an energy source (Kelly *et al.*, 2000). The organism was reclassified in 2000 from the genus *Thiobacillus* in the *Betaproteobacteria* to its own genus the *Starkeya* in the *alphaproteobacteria* due to new 16S rRNA analysis (Kelly *et al.*, 2000). This organism is a strict aerobe that oxidizes and grows on thiosulfate and tetrathionate (Kelly *et al.*, 2000).

Thiomicrospira crunogena EPR75 and *Halothiobacillus hydrothermailis* EPR 155 are hydrothermal vent organisms isolated from the East Pacific Rise at a diffuse flow vent based on their ability to aerobically oxidize thiosulfate (Crespo-Medina 2009). Both organisms are *Gammaproteobacteria* that can grow autotrophically on thiosulfate and heterotrophically with acetate (Crespo-Medina 2009).

Media. A mineral salts medium was used for *Bosea* sp. WAO and *Starkeya novella* experiments. To prepare one liter of medium 7.9 g $Na_2HPO_4 + 7H_2O$ and 1.5 g KH_2PO_4, 0.3 g NH_4Cl, 0.81 g $MgCl_2 + 6\ H_2O$, 5 mL VS mineral solution, 1 mL S8 vitamin solution, plus 10 mM bicarbonate. The VS minerals for a 200 mL stock were 10 g EDTA, 2.09 g $ZnCl_2 + H_2O$, 1.73 g $CaCl_2 + 2H_2O$, 1.6 g $MnCl_2 + 4H_2O$, 0.72 g $FeCl_2 + 4$ H2O, 0.22 g $(NH_4)_2Mo_7O_{24} + 4\ H_20$, 0.22 g $CuCl_2 + 2H_2O$, 0.32 g $CoCl_2 + 6H_2O$. The S8 vitamin stock for a 1 Liter is 2 mg Biotin, 2 mg folic

acid, 10 mg pyridoxine HCl, 5 mg riboflavin, 5 mg nicotinic acid, 5 mg pantothenic acid, 0.1 mg vitamin B12, 0.005 mg P-amino benzoic acid, and 0.005 mg thiocetic acid.

The saltwater medium used for *Thiomicrospira crunogena* EPR75 and *Halothiobacillus hydrothermailis* EPR 155 was recipe #142 from Deutsche Sammlung von Mikroorganismen und Zellkulturen (DSMZ) culture collection. The recipe was modified to use the same S8 vitamin stock in the mineral medium recipe above, 1 mL stock per Liter medium.

Culture Conditions. To determine if the four sulfur oxidizing organisms could grow by utilizing antimony compounds as their sole electron donor the organisms' growth and chemical transformations of the metal were monitored over time. Two sets of conditions: background control and active cultures were established for each media type and electron donor. The background controls in duplicate consisted of medium amended with 2 mM Sb(0) or 2 mM Sb(III) to examine if any abiotic transformations occurred. Active cultures in triplicate contained medium, microorganism, and 2 mM Sb(0) or Sb(III). Cultures were incubated in the dark at 30 °C on an orbital shaker to maximize aeration for 15 days.

At each time point samples were taken from all conditions and all replicates to analyze for Sb and growth. An aliquot of 0.8 mL was removed and immediately filtered through a Spin-X filter tube and frozen until chemical analysis using inductively coupled plasma mass spectrometry (ICP-MS). An

additional aliquot of 1 mL was removed and centrifuged to collect all insoluble components for protein analysis. The media was removed and MilliQ ultra-pure water was used to resuspended the insoluble components to the same volume for protein analysis. Protein analysis was completed using the Pierce BCA Protein Assay Kit from Thermo Scientific (Rockford, IL).

An additional set of cultures and controls were prepared to determine if any of the organisms could grow on the ligand sodium tartrate used to keep Sb(III) in solution. Triplicate cultures of each organism were amended with 2 mM sodium tartrate and monitored for growth using optical density (OD) measurements. Blank controls were set up for each medium with 2 mM sodium tartrate. OD measurements were taken periodically at 525 nm for 11 days.

Stibnite Oxidation. To examine if *Bosea* sp. WAO could oxidize sulfur bound in antimony sulfide, the production of sulfate from Sb_2S_3 was monitored over time. Experiments were conducted to determine the rate and extent of oxidation. Three sets of conditions: sterile control, background control, and active cultures were established with 2 mM Sb_2S_3, 2 mM sodium thiosulfate, or no electron donor. Sterile controls in duplicate contained minimal media, Strain WAO autoclaved three times, and 2 mM Sb_2S_3, 2 mM sodium thiosulfate, or no electron donor to determine if dead cellular material affected oxidation. The background controls in duplicate consisted of only the minimal salts medium, amended with 2 mM Sb_2S_3, 2 mM sodium thiosulfate, or no electron donor to examine if any abiotic transformations occur. Active cultures in triplicate

contained medium, Strain WAO, and 2 mM Sb_2S_3, 2 mM sodium thiosulfate, or no electron donor. Cultures were incubated in the dark at 30 °C on an orbital shaker to maximize aeration.

At each time point samples were taken from all conditions and all replicates to analyze for sulfate concentration. An aliquot of 0.8 mL was removed and immediately filtered through a Spin-X filter tube and frozen until analysis to prevent further oxidation of compounds.

Sulfate Analysis. Dissolved sulfate concentrations were determined using Ion chromatography on a Dionex® DX-120 with a Dionex Amms 300 suppressor. The guard column was a RFIC IonPac® AG14A 4 x 50 mm and the analytical column is an RFIC IonPac® AS14A 4x 250 mm.

Antimony Analysis. Samples from Sb(0) and Sb(III) tartrate experiments were diluted 1000 fold before analysis using deionized water (MilliQ ultra pure deionized, Millipore Corp, Billerica, MA). Standard solutions were prepared in 5 % HNO_3 (EMD omni trace ultra high purity, VWR) from a commercial antimony standard (High Purity Standards, N. Charleston, SC). Metal concentrations samples were quantified by inductively coupled plasma mass spectrometry on a Thermo-elemental X5 instrument (ThermoFisher Scientific). Table 4.1 lists the operating parameters. The concentrations for antimony were measured directly using calibration standard curves and fully quantitative analysis. QA/QC protocols were maintained throughout the analysis process including laboratory blanks, and a NIST traceable SRM (NIST A). This method has previously been used for

metals analysis in human serum samples (Xie *et al.*, 2007a), whole blood samples (Riedt *et al.*, 2009) and urine samples (Xie *et al.*, 2007b).

Results

The growth and activity of four different sulfur oxidizing microorganisms on two antimony compounds, Sb(III) and Sb(0), and the organic salt sodium tartrate, ($C_4H_4Na_2O_6$), were examined. No difference in optical density was observed between the controls lacking tartrate and the cultures with tartrate (Fig. 4.1). This indicated that under these conditions the organisms do not grow on tartrate alone. Growth on elemental antimony and antimonyl tartrate was monitored by change in protein concentration. In all cases for elemental antimony the initial protein concentration was higher than the final concentration indicating that the organisms died over the experimental period of fifteen days (Fig. 4.2). For antimony tartrate only *Halothiobacillus hydrothermailis* EPR 155 showed a slight increase in protein concentration. However, the standard deviation indicated that the difference between the two points was not outside of experimental variability (Fig. 4.3).

The total soluble antimony that could be in oxidation states 0, +3, or +5 was measured using ICP-MS. This analysis could not determine the oxidation state, only the concentration of Sb present in the aqueous phase. Elemental Sb(0) is insoluble in water so initial concentrations were expected to be low. The Sb(III) bound to tartrate is soluble and therefore should measure the same as

the initial Sb(III) concentration added to the experiment. Change in solubility was used as a proxy indicator for the microbial oxidative activity when compared to background controls (BG) that contained only Sb and medium.

Total soluble antimony from the saltwater microorganisms *Thiomicrospira crunogena* EPR75 (T1) and *Halothiobacillus hydrothermailis* EPR 155 (H1) replicate one Sb(0) samples have a slight increase in solubility, however the increase occurs in both background and active samples suggesting it is an abiotic reaction (Fig. 4.4). For the Sb(III) samples, the loss of soluble Sb occurs in both the active and background control samples suggesting that the loss is due to abiotic processes.

Total soluble antimony from the freshwater microorganisms *Bosea* sp. WAO (W1) and *Starkeya novella* (S1) replicate one results are shown in Figure 4.5. The results for Sb(0) is consistent across all samples with a slight increase in solubility over time. Since this is evident in the background and active cultures this suggests the process is due to abiotic reactions. For the Sb(III) samples the *Starkeya novella* (S1) active and the BG1 both show a decrease in solubility. In the *Bosea* sp. WAO (W1) samples the solubility seems to remain consistent over the time period sampled. This suggests that the microbes might have an effect on the Sb(III). Analysis of two additional replicates of *Bosea* sp. WAO show that replicates W2 and W3 follow the same trend as the rest of the microorganisms and the background decreasing in solubility over time (Fig. 4.6). This suggests that the W1 sample is an outlier that does not match the rest of the data set.

Therefore, the change in solubility is again due to abiotic processes and not due to WAO.

An additional set of experiments were run with *Bosea* sp. WAO using antimony sulfide and sodium thiosulfate as electron donors. WAO is able to quickly oxidize all the available thiosulfate to sulfate (Fig. 4.7). No sulfate is produced in the sterile controls, backgrounds, or no e- donor added samples indicating that the sulfate produced in the active culture is due to biological activity. The active cultures with antimony sulfide show an initial rate of sulfate productions of 0.32 mM/day compared to much lower rates of the background controls at -0.006 mM/day and sterile controls at 0.03 mM/day. However, when we look at the total percent sulfate oxidized the active cultures reach 100 % and then decrease to the same levels as the controls (Fig. 4.8). This suggests that the microorganism may be speeding up the oxidation but that other additional processes are also taking place.

Discussion

Bosea sp. WAO, *Starkeya novella*, *Thiomicrospira crunogena* EPR75 and *Halothiobacillus hydrothermailis* EPR 155 were tested and determined to be unable to grow on sodium tartrate (Fig. 4.1). This is important as studies looking at microbial growth and oxidation of soluble antimony use potassium antimonyl tartrate as their election donor (Lehr *et al.*, 2007, Li *et al.*, 2013). The tartrate can be a potential carbon source for heterotrophic growth. By selecting for

organisms that are unable to use tartrate we show that any growth observed on the antimony compounds would be due to oxidation of the antimony and not the associated ligand. When the organisms were incubated with Sb(0) and Sb(III) no apparent growth was observed (Fig. 4.2 and Fig. 4.3). This suggests that the organisms are incapable of using these compounds as electron donors for chemolithoautotrophic growth. Two other studies reported growth on antimonyl tartrate; however, the investigators grew their organisms in media amended with mannitol or lactate and not under strict autotrophic conditions (Lehr *et al.*, 2007, Li *et al.*, 2013). An additional study using radioisotope labeled [^{14}C]-bicarbonate, antimonyl tartrate and *Variovoraz paradoxus* strain IDSBO-4 did show incorporation of the labeled carbon suggesting chemoautotrophy; however, the organism was also shown to grow on tartrate in the absence of antimony (Terry *et al*., 2015). This leaves open the possibility that growth in these reports might still be heterotrophic with the microbes using the organic ligand or other organic compounds in the medium. In my studies I also determined that the organisms were not changing the solubility of Sb(0) or Sb(III) when compared to the background controls (Fig. 4.4 and Fig. 4.5). This supports my conclusion that these microorganisms are not interacting with the different antimony species.

Bosea sp. WAO was able to initially stimulate the release of sulfate from stibnite at a faster rate than background or sterile controls. However, after sulfate production peaked the total soluble concentration decreased and eventually overlapped with the background or sterile controls sulfate

concentration (Fig. 4.8). This organism has been previously shown to be able to oxidize arsenopyrite, sodium arsenite and several reduced sulfur compounds to release stoichiometric amounts of sulfate into solution, however, in this case the sulfate produced from stibnite was not maintained in the aqueous phase. This could be happening for several reasons. 1) The addition of phosphate reacts with the mineral and WAO takes advantage of bioavailable sulfur produced like it does with PbS (Chapter 3) and; therefore, in the absence of WAO the phosphate reacts with the mineral and the sulfur released is more slowly oxidized abiotically to sulfate. 2) The production and then decrease of sulfate from the stibnite is due reason one (1) plus the abiotic reaction of the sulfate reacting with the available antimony to precipitate as the mineral antimony sulfate. 3) Phosphate is not involved with the reaction and WAO does directly oxidize stibnite until a point where the antimony is toxic and/or the sulfate starts reacting back onto the original mineral. Additional tests would be required to tease these options apart such as XRD to see how the mineral is changing.

Studies using stibnite ore have focused on organisms that oxidize the sulfur at low pH making the mineral more soluble and the sulfide more accessible to the organisms (Torma and Gabra 1977, Tsaplina *et al.*, 2010, Zhuravleva *et al.*, 2011). Additionally, although antimony is chemically similar to arsenic, it was recently shown that a mutant strain incapable of its normal arsenic oxidation ability was still able to oxidize antimony indicating that the arsenic *aio* oxidation pathway for chemotrophic growth was not required for antimony oxidation (Lehr

et al., 2007). This supports the notion that not all arsenic oxidizers will be able to also oxidize antimony.

Conclusions

Biogeochemical cycling of minerals is highly dependent on the environmental conditions present. Here we clearly show that these organisms are incapable of using the organic carbon ligand for growth and are not growing on Sb(III) or Sb(0). Studies that utilize tartrate must be careful to determine that the organisms are not actually growing on the tartrate or other carbon sources added into the medium. In studies were the organisms are able to grow on the tartrate observed changes in oxidation state may be due to detoxification activities rather than for growth. Studies of microbial stibnite oxidation may be observing oxidation of antimony in stibnite only as a byproduct of sulfide oxidation by acid mine drainage organisms that are highly adapted to obtaining the sulfur. Continued work looking at the mineral transformation may elucidate if the sulfate is released into the environment or retained on the mineral surface. Additional studies that tease apart the sulfur oxidation and antimony oxidation by using antimony trioxide will help to elucidate if the oxidation is actually due to microbial activity.

Figures

Table 4.1. Instrumental Parameters for Antimony Analysis

Parameter	Value
Cones	Nickel
Spray chamber	Impact bead (Ionflight, Charlestown, MA)
Nebulizer	1 mL/min concentric, (Glass Expansion, Pocasset, MA)
Autosampler	Cetac ASX510
RF power	1230 W
Cool gas flow	13 L/min
Auxiliary gas flow	0.83 L/min
Nebulizer gas flow	0.91 L/min
Dwell time	82 ms
Acquisition time	18 ms
Replicates	3

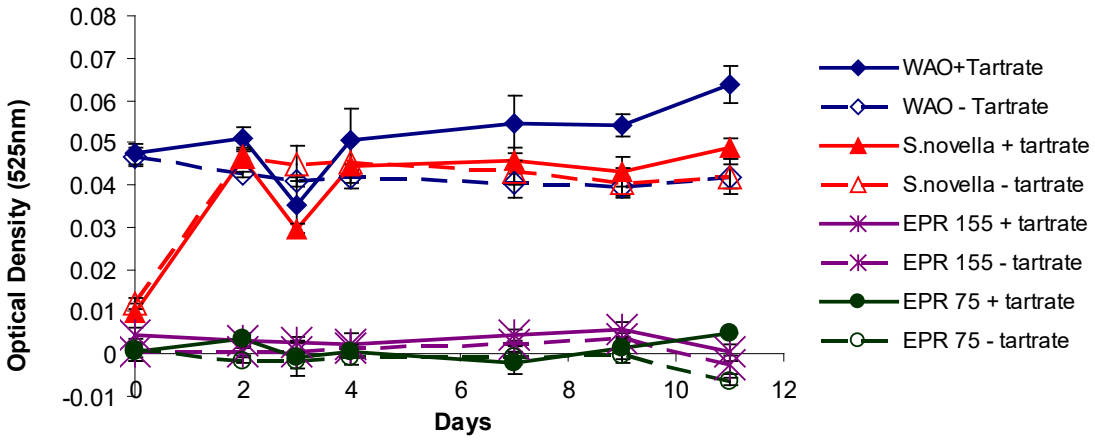

Figure 4.1. Growth on tartrate was determined by measuring optical density at 525 nm. Cultures were set up in triplicate for each organism +/- the addition of 2 mM sodium tartrate. Solid lines (+) tartrate, dashed lines (-) tartrate.

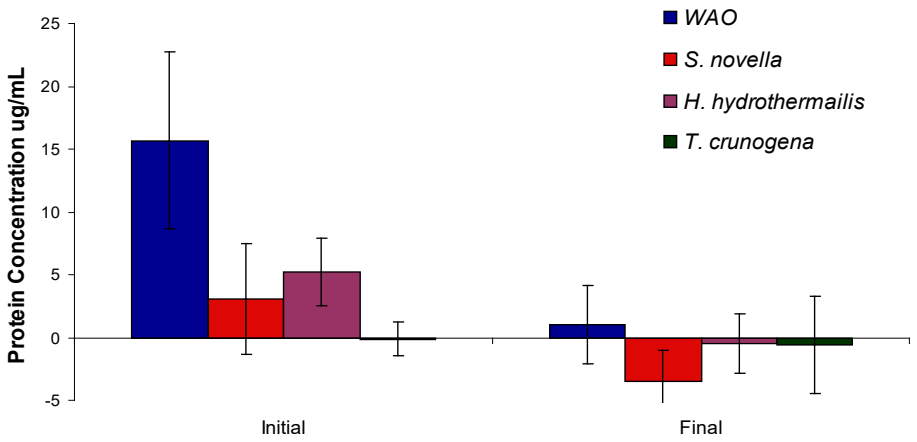

Figure 4.2. Growth on the electron donor Sb(0). Growth of organisms on Sb(0) at the initial time point and final time point 15 days later monitored by protein concentration. Error bars indicate the standard deviation between three replicates.

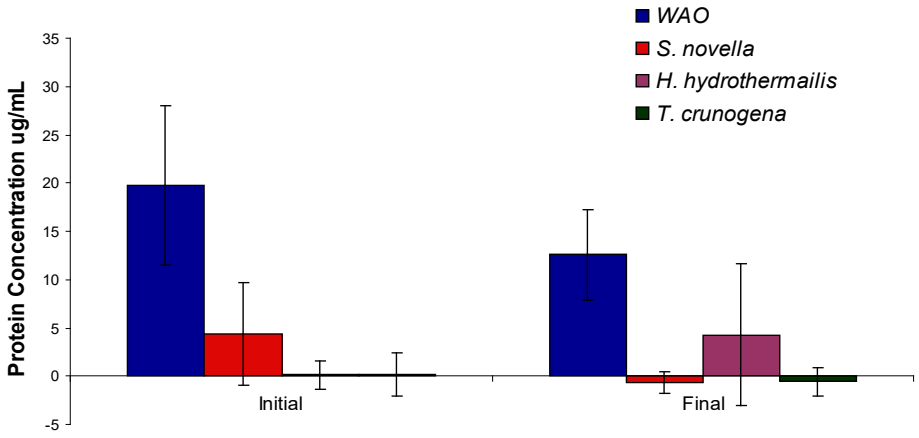

Figure 4.3. Growth on the electron donor Sb(III) as antimony tartrate. Growth of organisms on Sb(III) at the initial time point and final time point 15 days later monitored by protein concentration. Error bars indicate the standard deviation between three replicates.

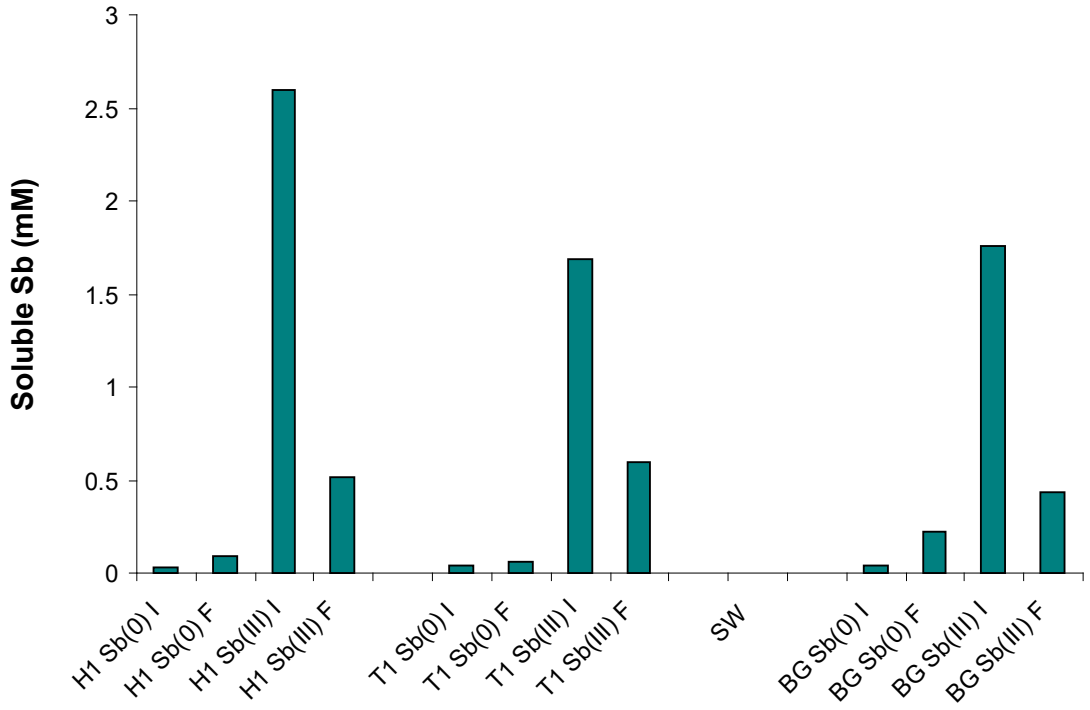

Figure 4.4. Soluble Antimony from Saltwater organisms. Concentration of total soluble Sb from saltwater organism cultures *Thiomicrospira crunogena* EPR75 (T1), *Halothiobacillus hydrothermailis* EPR 155 (H1), media alone (SW), and background control (BG). Results shown are from one of three replicates at an initial (I) and final time point (f) after 15 days of incubation.

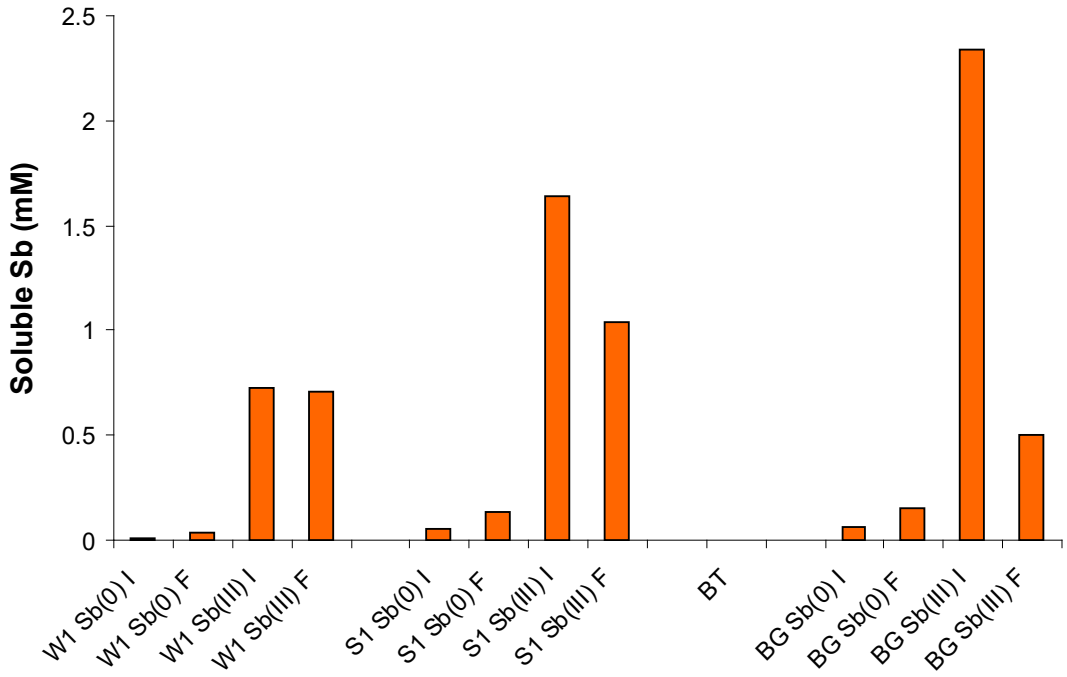

Figure 4.5. Total soluble antimony from freshwater organisms. Concentration of total soluble Sb from freshwater organisms *Bosea* sp. WAO (W1), *Starkeya novella* (S1), media alone (BT), and background control (BG). Results shown are from one of three replicates at an initial (I) and final time point (f) after 15 days of incubation.

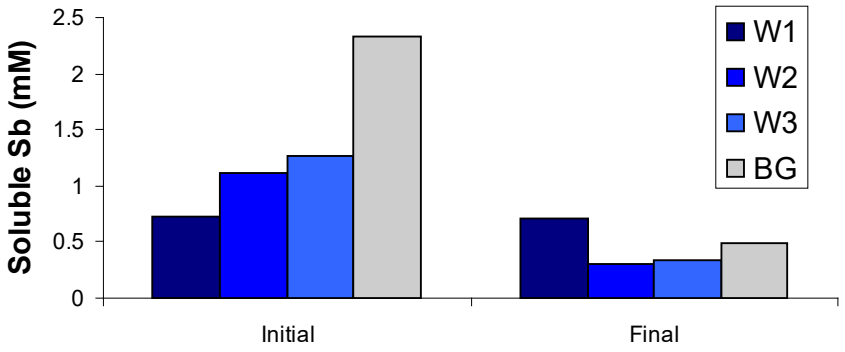

Figure 4.6. Concentration of total soluble Sb from additional replicates of freshwater organism *Bosea* sp. WAO (W1) and background control (BG). Results shown are of three replicates at an initial and final time point after 15 days of incubation.

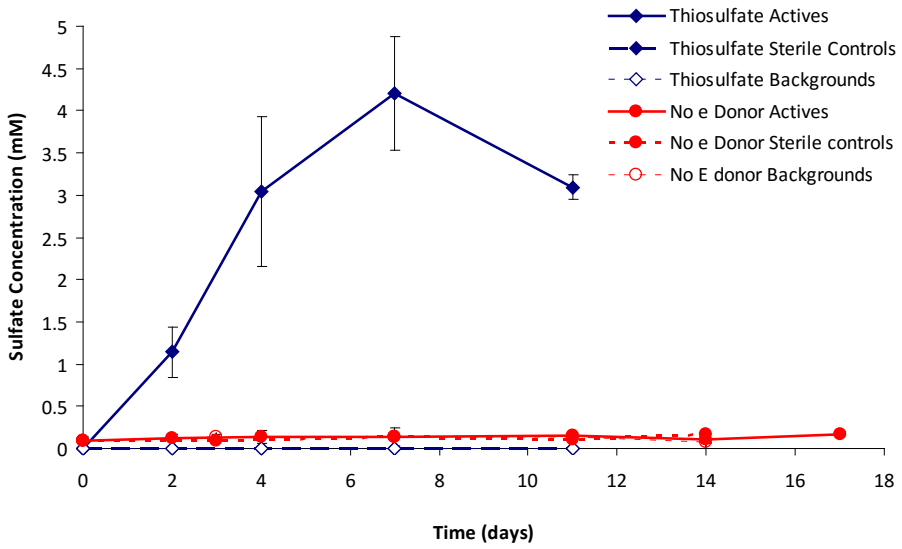

Figure 4.7. Sulfate produced by *Bosea* sp. WAO from the oxidation of the positive control electron donor thiosulfate in comparison to the addition of no electron donor. Actives in triplicate contain WAO, steriles in duplicate have killed WAO, and backgrounds in duplicate have no cells added. Error bars are the standard deviation of the replicates.

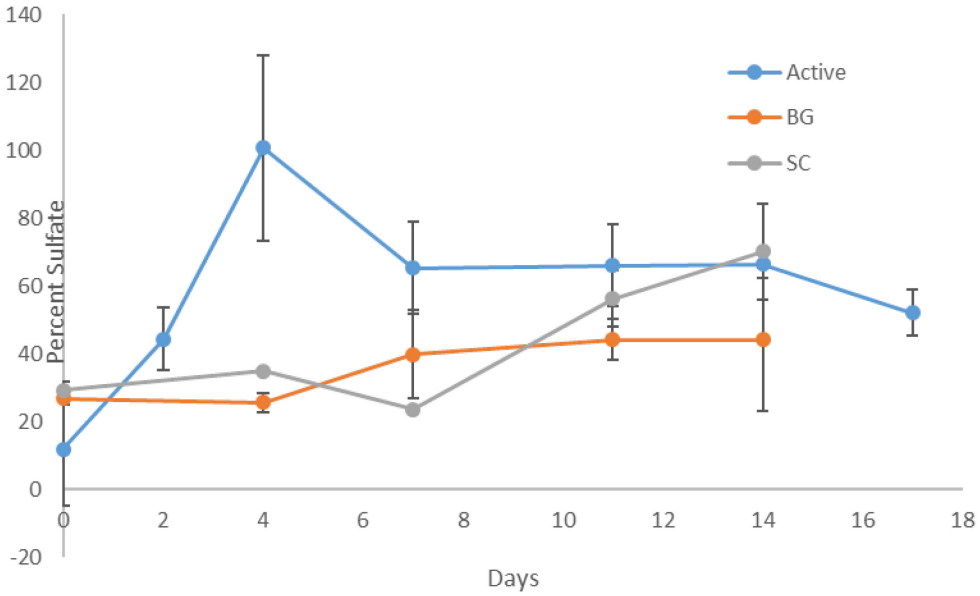

Figure 4.8. Percent sulfate produced by *Bosea* sp. WAO from the oxidation of stibnite. Actives in triplicate contain WAO, steriles (SC) in duplicate have killed WAO, and backgrounds (BG) in duplicate have no cells added. Error bars are the standard deviation of the replicates.

Chapter 5:

Conclusions and Future Directions

Microorganisms and their metabolic capabilities have had a significant role in shaping the biosphere (Ehrlich 1996, Gadd 2010, Konhauser 2007). Microbial metabolism can impact the redox chemistry of soil environments leading to the leaching and solubilization or stabilization of metals and other soil components (Gadd 2010). Chemosynthetic microorganisms can grow by utilizing a wide range of inorganic substrates such as sulfur or metals to obtain energy for carbon fixation (Shively *et al.*, 1998). Anthropogenic activities modify soil environments, changing the redox chemistry and thus the availability of compounds for these chemosynthetic organisms to use.

The main objective was to explore microbe-mineral interactions at circumneutral pH using minerals as possible electron donors for the growth of a model facultative chemolithoautotrophic microorganism *Bosea* sp. WAO. This organism's genome was sequenced and studied for functional genes related to chemolithoautotrophic growth. The organism's metabolic capabilities for the utilization of the electron donors PbS, Sb(III), Sb(0), and Sb_2S_3 were determined. Three additional chemolithoautotrophic sulfur oxidizers were studied for growth on Sb(III) and Sb(0).

In Chapter 2 I built upon previous work to further characterize *Bosea* sp. WAO through physiological studies and an analysis of the newly sequenced genome. Previously *Bosea* sp. WAO was shown to oxidize arsenite and reduced

sulfur compounds for chemolithoautotrophic growth in addition to being capable of heterotrophic growth (Rhine *et al*., 2008). During these original studies only the genes for the arsenite oxidation pathway (*aioA*) and carbon fixation pathway (RuBisCO) were amplified by traditional PCR (Rhine *et al*., 2008).

Growth of *Bosea* sp. WAO occurs at an optimal temperature range between 20-35 °C. *Bosea* sp. WAO grows between pH 5-9.5 with the optimal range at pH 8-8.5, while at more acidic pH values below 5.5 there is a significant delay in the start of exponential growth phase. No growth is observed below pH 4.5. Growth over a range of salinities was tested with no growth observed over 3.5 % w/v NaCl.

From the analysis of the incomplete draft genome of 6,125,776 bp it was determined that *Bosea* sp. WAO has a GC content of 66.84 %, 62 RNA genes, and a predicted 5,727 genes of which 5,665 or 98.92 % are protein coding. The genus *Bosea* has nine species with validly published names with the highest 16S rRNA pairwise similarities found with the type strains *B. vestrisii* 34635^T (99.72 %), *B. eneae* 34614^T (99.65 %), *B. lupini* R-45681^T (99.65 %), *B. thiooxidans* BI-42^T (99.24 %), *B. robiniae* R-46070^T (98.88 %), *B. massiliensis* 63287^T (98.81 %), *B. minatitlanensis* AMX51^T (98.48 %) and *B. lathyri* R-46060^T (98.18 %) (Kim *et al*., 2012). Phylogenetic analysis based on the 16S rRNA gene of *Bosea* spp. and phylogenetically related organisms placed *Bosea* sp. WAO closest to the type strain *B. lupini* DSM 26673^T, with *B. vestrisii* 34635^T and *B. eneae* 34614^T in the same cluster. An average nucleotide identity analysis (ANI)

score between strain WAO and *B. lupini* DSM 26673^T was 84.64 % which is lower than the ANI species demarcation threshold range (95-96 %) (Kim *et al*., 2014). The ability of *B. lupini* to oxidize thiosulfate has not been determined (De Meyer *et al*., 2012); however, both *B. vestrisii* 34635^T and *B. eneae* have been determined to not oxidize thiosulfate to sulfate (La Scola *et al*., 2003). These results suggest that strain WAO represents a distinct species in the genus *Bosea*.

Bosea sp. WAO is able to grow under chemolithoautotrophic conditions with arsenite and thiosulfate in addition to growing under heterotrophic conditions. Analysis of the genome herein revealed that the arsenite oxidation pathway was complete with *Bosea* sp. WAO possessing genes for both the small subunit, *aioB*, and reconfirming the large subunit, *aioA*. Analysis for the remaining genes of the Calvin-Benson-Bassham Cycle for carbon fixation indicated that all of the required genes were present. Additionally, *Bosea* sp. WAO possesses all the necessary genes necessary in the *sox* pathway for to allow for complete oxidation of S_2O_3 to SO_4^{2-}. When nutrient conditions are low, this organism can oxidize reduced sulfur compounds and arsenite, impacting the oxidative halves of the biogeochemical cycle for both of these elements.

Future work with the WAO genome should include closing the gaps in the genome as currently only two complete genomes, *Bosea thiooxidans* CGMCC 9174 V5_1 and *Bosea vaviloviae* strain SD260*,* exist for the *Bosea* genus. Additional comparisons between these compete genomes would allow for further elucidation of potentially missing or partial pathways in WAO. Additionally, the

development of new primer sets to probe environmental samples for sulfur compound oxidation would also be useful as current primers only work on a subset of organisms and were unable to amplify sequences of interest in this organism. These primers could be used on environmental samples or to probe metagenomic data looking for related genes in other organisms. This type of *in silico* approach to probing metagenomic samples for similar chemolithoautotrophic pathways will allow for the development of targeted enrichment cultures from those environments. Additional work on this organism's physiology can be guided by exploring pathways elucidated by the genomic analysis. This guided physiological characterization will allow us to show both the presence and activity of the genes involved.

In Chapter 3 I explored how microorganisms can change mineral composition during substitution reactions. The aqueous concentration of lead (Pb) in geochemical environments is controlled by the solubility of Pb-bearing minerals and their weathering products. In contaminated soils, a common method for *in situ* stabilization of Pb is the addition of phosphate to convert more redox sensitive sulfide minerals into the sparsely soluble pyromorphite ($Pb_5(PO_4)_3X$) where X= Cl, Br, F, or OH (Ruby *et al.*, 1994, Zhang and Ryan 1999, Martinez *et al.*, 2004, Kumpiene *et al.*, 2008, Scheckel *et al.*, 2013). In this study I determined the fate of the bound sulfur during the conversion of galena (PbS) to pyromorphite after the addition of soluble phosphate. Powder X-ray diffraction analysis indicated that the secondary mineral precipitate was chloropyromorphite

($Pb_5(PO_4)_3Cl$) and elemental sulfur (S_8). In abiotic controls only a small amount of sulfur was present in the aqueous phase as sulfide, thiosulfate, or sulfate. Together, the data indicate that during the conversion of galena to pyromorphite, sulfide is abiotically oxidized to elemental sulfur which is retained in the solid phase. However, when PbS reacted in the presence of *Bosea* sp. WAO the S_8 in the secondary mineral was oxidized to sulfate. *Bosea* sp. WAO produced significantly more sulfate from the secondary mineral than from the primary galena. I believe the oxidation results of this study show that stimulation of sulfur-oxidizing organisms may be a direct consequence of phosphate amendments to Pb contaminated soils. Furthermore, understanding these complex interactions allows for improved modeling of both the geochemical and biological aspects of lead sulfide mineral transformation in contaminated sites.

Future studies should explore how the concentration and form of the phosphate added to the system changes the rate and extent of formation of sulfur and the ability of *Bosea* sp. WAO to access the reduced sulfur. Sulfide oxidizing microorganisms that favor circumneutral conditions produced by the phosphate amendment buffering the system will thrive until the buffering capability is surpassed. In the case of organisms intolerant to acidic pH like *Bosea* sp. WAO growth will be inhibited once the pH drops below 4.5. Other more acidophilic organisms may begin to take over once those conditions are reached which could cause a release of other acid soluble co-contaminants into the environment. It will be important to model how much phosphate will be

required to keep the system buffered and prevent the possible release of other contaminants. These additional studies may determine that it is important to limit phosphate amendments to sites where lead contamination bound in non-sulfur minerals such as cerussite ($PbCO_3$) or Pb-salts such as $Pb(NO_3)_2$. In these situations, this will eliminate the secondary sulfur reactions that produce sulfate.

Another interesting area of future study could be the intersection of phosphate contamination and historical Pb contamination in freshwater streams. Excess phosphate from fertilizer runoff and wastewater treatment plant effluent enters ground water and surface water potentially causing eutrophication which leads to the stimulation of plants and algae causing a bloom (Chislock *et al.*, 2013). As the bloom dies off bacteria aerobically degrade the algae depleting the oxygen and causing hypoxic or anoxic zones which kill off larger organisms such as macroinvertebrates and fish (Chislock *et al.*, 2013). Thus, it would be interesting to examining areas where these contamination sources overlap to determine if the phosphate runoff reacts with the Pb and if so, is it reducing Pb bioavailability. This situation could be envisioned in regions where more rural or suburban areas exist upstream from heavily developed and industrialized areas. In this case the two contamination sources could be neutralizing one another, improving water quality downstream from their interaction.

In Chapter 4 I explored the ability of four sulfur oxidizing chemolithoautotrophic microorganisms to oxidize antimony compounds at neutral pH. The concentration of antimony in sediment pore water is limited by the

solubility of its compounds. Most naturally occurring antimony compounds are highly insoluble at neutral pH and require acids to increase solubility. This would limit the exposure of neutrophilic organisms to dissolved antimony except at contamination sites that have higher dissolved levels due to higher overall concentrations present in the area. *Bosea* sp. WAO, *Starkeya novella*, *Thiomicrospira crunogena* EPR75 and *Halothiobacillus hydrothermailis* EPR 155, all unable to utilize sodium tartrate as a carbon source, were used to study growth on the electron donors potassium antimonyl(III) tartrate and elemental antimony(0). None of the microorganisms were able to grow on either elemental or potassium antimonyl tartrate under strict autotrophic conditions. *Bosea* sp. WAO was initially able produce sulfate from stibnite, (Sb_2S_3) the most common form of antimony in the environment, at a faster rate than background or sterile controls. However, with additional time this rate decreased and final total soluble sulfate concentrations were the same for all conditions within experimental error.

We clearly show that the microorganisms tested in this study are incapable of using the organic carbon ligand, tartrate, for growth and are not growing on Sb(III). Previous studies that utilized tartrate or amended the medium with other carbon sources did not address the possibility of heterotrophic conditions as the reason for growth (Lehr *et al.*, 2007, Li *et al.*, 2013). Terry *et al.*, 2015 determined that the organisms were able to grow on the carbon ligand making it difficult to resolve whether observed changes in oxidation state of Sb are due to detoxification or for growth. The insolubility of

stibnite makes it difficult for circumneutral microorganisms to access the sulfide present, however in my experiment *Bosea* sp. WAO did initially increase the rate of sulfate release. Earlier studies (Torma and Gabra 1997, Tsaplina *et al.*, 2010, Zhuravleve et al., 2011) may be seeing oxidation of antimony in stibnite only as a by product of sulfide oxidation. These acid mine drainage organisms are highly adapted to obtaining the sulfur under acidic conditions and may be only releasing the Sb that is oxidized abiotically.

Future studies to tease apart the sulfur oxidation and antimony oxidation can be facilitated by using antimony trioxide to elucidate whether the oxidation of antimony in experiments with these organisms is due to direct microbial activity and not a byproduct of the microbial sulfur oxidation. Utilizing antimony trioxide instead of the organic ligand containing compound antimony tartrate will also clarify if growth is due to heterotrophic or autotrophic metabolism. The main difficulty with studying antimony compounds is their insolubility. Further exploration of these Sb redox changes using insoluble compounds will require the development of new analytical chemistry methods that are able to measure the oxidation state of the insoluble antimony compounds are required.

Additional future work that explores why there is a difference in the initial production rate of sulfate from stibnite would need to tease apart the chemical and biological activity. This could be happening for several reasons. 1) The addition of phosphate reacts with the mineral and WAO uses the more bioavailable sulfur as it does with PbS (Chapter 3) and; therefore, in the absence

of WAO the phosphate reacts with the mineral and releases sulfur which is more slowly abiotically oxidized to sulfate. 2) The production and then decrease of soluble sulfate from the stibnite is due to reason (1) plus the abiotic reaction of the sulfate reacting with the available antimony and precipitating to produce the mineral antimony sulfate. 3) Phosphate is not involved with the reaction and strain WAO does directly oxidize stibnite until a point where the antimony is toxic and/or the sulfate starts reacting with the original mineral. Monitoring the change in mineral composition over time with XRD with conditions varying both the presence and absence of WAO and phosphate will allow for the differentiation of several of these possibilities. To see if toxicity is an issue the starting concentration of antimony can be varied under heterotrophic conditions to determine at which point growth is inhibit and then future experiments can be run below the minimal inhibitory concentration (MIC).

Microorganisms perform complex metabolic interactions with the minerals surrounding them to fulfill their requirements for growth or for detoxification. These interactions alter the redox conditions thus affecting the geochemical cycling of elements. My research adds to the expanding field of geomicrobiology as more and more evidence shows that microorganisms are the primary weathering agents of mineral surfaces through the dissolution and mobilization of mineral components. Here I have explored interactions with minerals containing sulfur and arsenic, both of which are readily used as electron donors for growth from both soluble and insoluble sources. Although genes for many of

these pathways have been elucidated, the interactions and preference for one electron donor over another under environmentally relevant conditions is still unclear. Future work can continue to identify if microorganisms choose their electron donors solely on the energy available or some other preference such as protein binding potentials or diffusion through the cell membrane. Expanding our knowledge of geologic interactions among microorganisms brings us closer to learning possible signatures of early life on this planet and others.

This research also explored how remediation efforts need to take a multi-disciplinary approach to solving environmental problems. For instance, where normally a problem might be tackled using a single engineering approach, adding in biology and chemistry to solve a problem could be more comprehensive. Remediation techniques that manipulate the environment could enrich for unexpected biological activity or chemical transformations due to secondary reactions and the interactions between biology and the environmental chemistry. Furthering our understanding of how microbes interact with and modify the geology around them will improve our understanding of complex role microbes have in biogeochemical processes.

Appendix to Chapter 3

Supplemental Data: Gibbs free Energy Calculations

The Gibbs Free Energy calculations for the PbS to pyromorphite transformation were determined using ΔG° values from Stumm and Morgan 1981 and Nriagu 1974. Non-ideal effects were assumed to be negligible and activity coefficients were set to γ=1.

The value obtained from Gibbs Free Energy of the reaction was used to calculate in the free energy change under given initial conditions, ΔG using equation 1.

$$\Delta G = \Delta G^\circ + 2.303RT\log Q \qquad (1)$$

In equation (1) R is the universal gas constant, 0.008314 kJ/molK, K is the absolute temperature in Kelvin, and Q is the reaction quotient for the given initial conditions.

$$5PbS + 3HPO_4^{2-} + Cl^- + 5O_2 + 7H^+ \rightarrow Pb_5(PO_4)_3Cl + 5S^0 + 5H_2O$$

$\Delta G^\circ_{rxn} = \Sigma\Delta G^\circ_f$((-3791.54 kJ/mol) + (5*-237.18 kJ/mol))
- $\Sigma\Delta G^\circ_f$((5*-98.7 kJ/mol)+(3*-1089.3 kJ/mol)+(-131.3 kJ/mol))

ΔG°_{rxn} = -1084.74kJ/mol

$$Q = \frac{1}{[HPO_4^{2-}]^3[Cl^{1-}][O_2]^5[H^+]^7}$$

Calculated with the initial experimental conditions of T= 30 °C, $[O_2]$ = 0.234 mM, $[PO_4^{2-}]$ = 40 mM, $[Cl^-]$ = 7.86 mM, and pH = 7.3 is still favorable with a ΔG = -646.29 kJ/mol. Additional graphs were calculated by varying one parameter at a time in the quotient equation. It was determined that this mineral transformation reaction is energetically favorable in oxic neutral pH waters containing phosphate and chloride.

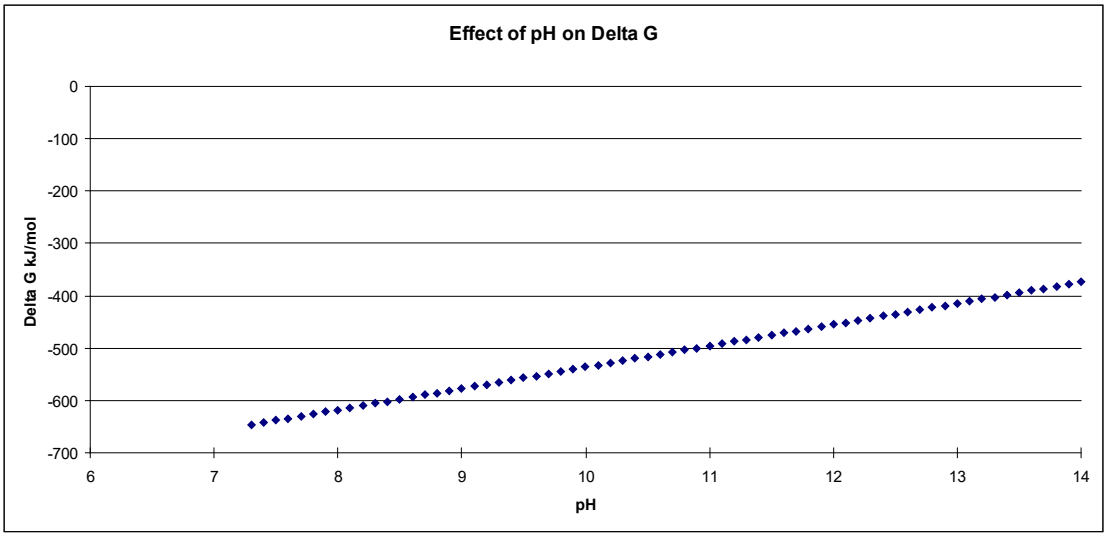
Effect of pH on Delta G
Delta G kJ/mol
0
-100
-200
-300
-400
-500
-600
-700
6
7
8
9
10
11
12
13
14
pH

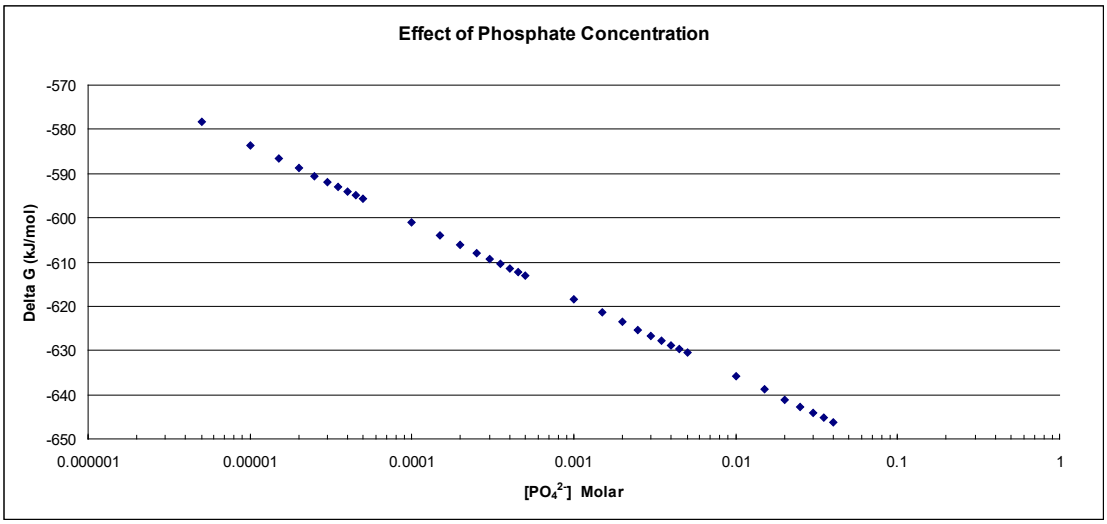
Effect of Phosphate Concentration
Delta G (kJ/mol)
-570
-580
-590
-600
-610
-620
-630
-640
-650
0.000001
0.00001
0.0001
0.001
0.01
0.1
1
[PO4 2-] Molar

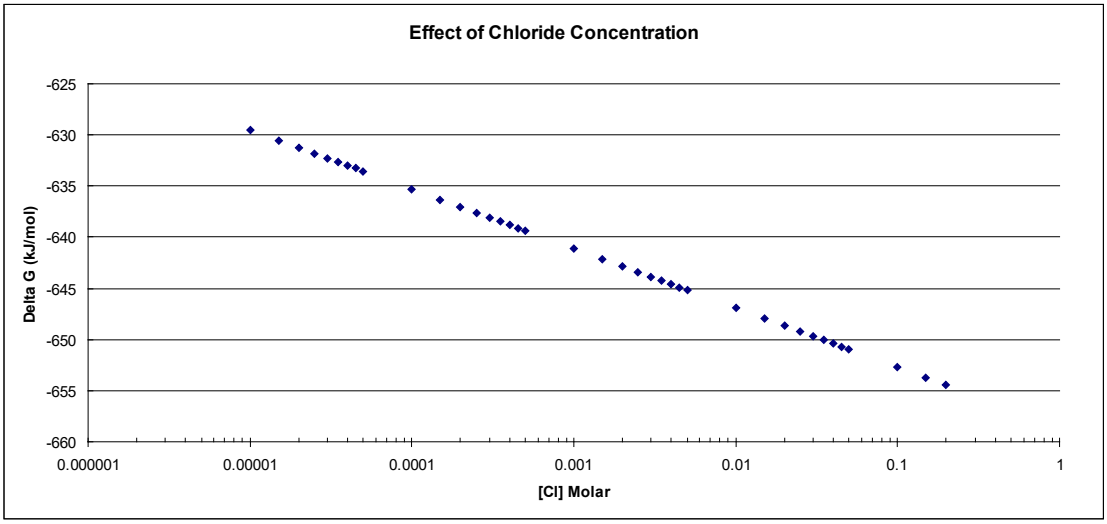
Effect of Chloride Concentration
Delta G (kJ/mol)
-625
-630
-635
-640
-645
-650
-655
-660
0.000001
0.00001
0.0001
0.001
0.01
0.1
1
[Cl] Molar

The Gibbs Free Energy calculations for the elemental sulfur oxidation under oxic conditions were determined using ΔG° values from Stumm and Morgan 1981. Non-ideal effects were assumed to be negligible and activity coefficients were set to γ=1.

$$S_{(s)} + 1.5O_{2(aq)} + H_2O \rightarrow SO_4^{2-} + 2H^+$$

$\Delta G°_{rxn} = \Sigma \Delta G°_f(-744.6 \text{ kJ/mol}) - \Sigma \Delta G°_f(-237.18 \text{ kJ/mol})$

$\Delta G°_{rxn} = -507.42 \text{ kJ/mol}$

$$Q = \frac{[SO_4^{2-}][H^+]^2}{[O_2]^{1.5}}$$

Calculated with the initial experimental conditions T= 30 °C, $[O_2]$ = 0.236 mM, $[SO_4^{2-}]$ = 2 μM and pH = 7.3 the reaction is more favorable with a ΔG = -593.67 kJ/mol. Additional graphs were calculated by varying one parameter at a time in the quotient equation. This reaction is energetically favorable at more basic pH values, high oxygen concentration and low sulfate concentration.

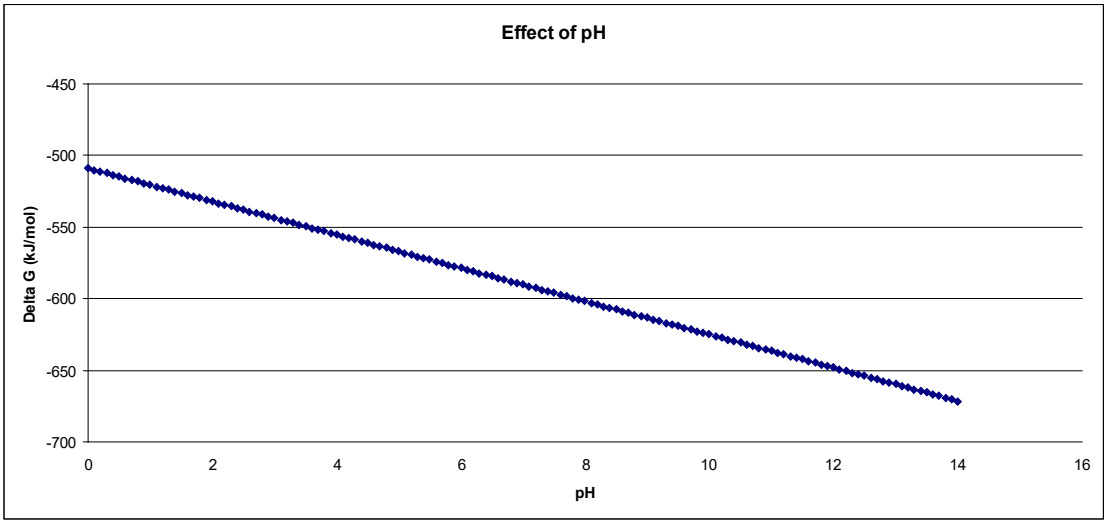

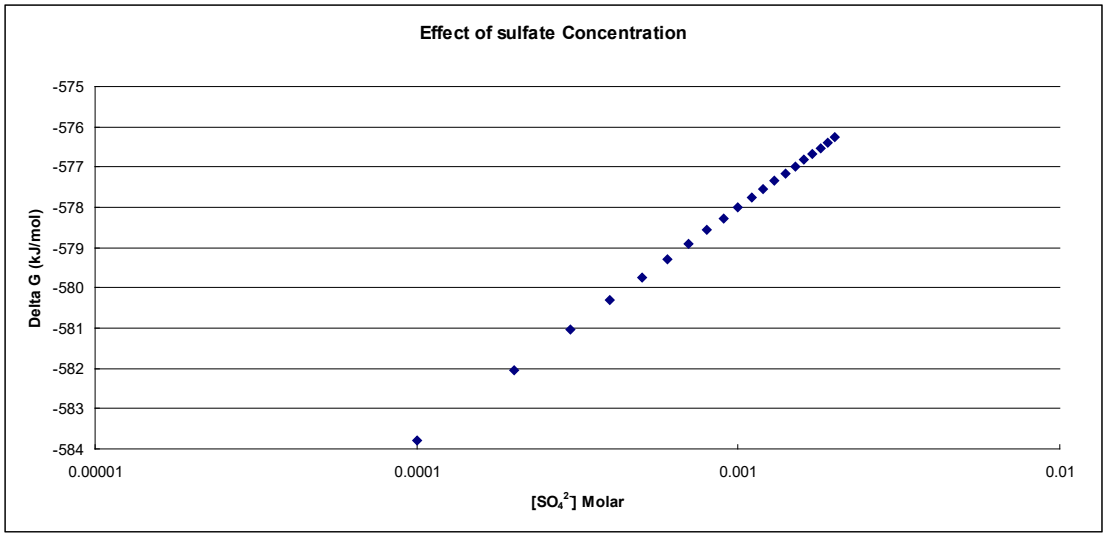
Effect of sulfate Concentration
Delta G (kJ/mol)
-575
-576
-577
-578
-579
-580
-581
-582
-583
-584
0.00001
0.0001
0.001
0.01
[SO4 2-] Molar

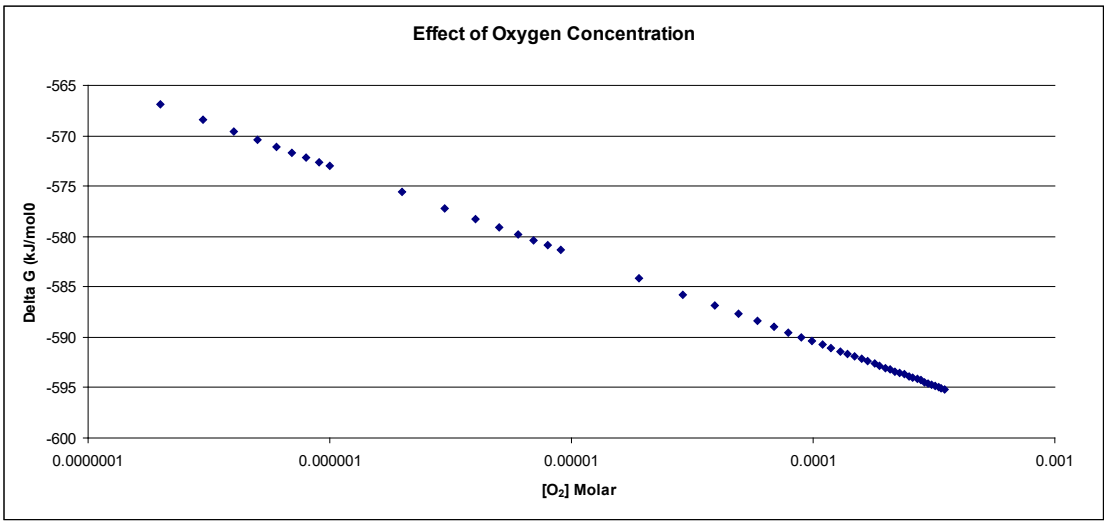
Effect of Oxygen Concentration
Delta G (kJ/mol0
-565
-570
-575
-580
-585
-590
-595
-600
0.0000001
0.000001
0.00001
0.0001
0.001
[O2] Molar

References

Adadin H, Ashizawa A, Stevens YW, Llados F, Diamond G, Sage G, Citra A, Quinones A, Bosch S, Swarts SG (2007) Toxicological profile for lead*. U.S. Dept. of Health and Human Services,*

Amend JP, Saltikov C, Lu G, Hernandez J (2014) Microbial arsenic metabolism and reaction energetics*. Reviews in Mineralogy and Geochemistry,* **79,** 391-433.

Atomi H (2002) Microbial enzymes involved in carbon dioxide fixation*. Journal of Bioscience and Bioengineering,* **94,** 497-505.

Aziz R, Bartels D, Best A, DeJongh M, Disz T, Edwards R, Formsma K, Gerdes S, Glass E, Kubal M, Meyer F, Olsen G, Olson R, Osterman A, Overbeek R, McNeil L, Paarmann D, Paczian T, Parrello B, Pusch G, Reich C, Stevens R, Vassieva O, Vonstein V, Wilke A, Zagnitko O (2008) The RAST Server: Rapid Annotations using Subsystems Technology*. BMC Genomics,* **9,** 75.

Baker BJ, Banfield JF (2003) Microbial communities in acid mine drainage*. FEMS microbiology ecology,* **44,** 139-152.

Bang SS, Deshpande SS, Han KN (1995) The oxidation of galena using *Thiobacillus ferrooxidans. Hydrometallurgy,* **37,** 181-192.

Berg IA (2011) Ecological aspects of the distribution of different autotrophic CO_2 fixation pathways*. Applied and Environmental Microbiology,* **77,** 1925-1936.

Bissen M, Frimmel FH (2003) Arsenic -- a Review. Part I: Occurrence, toxicity, speciation, mobility*. Acta Hydrochimica et Hydrobiologica,* **31,** 9-18.

Bowell RJ, Alpers CN, Jamieson HE, Nordstrom DK, Majzlan J (2014) The environmental geochemistry of arsenic — An Overview —*. Reviews in Mineralogy and Geochemistry,* **79,** 1-16.

Boyd ES, Druschel GK (2013) Involvement of intermediate sulfur species in biological reduction of elemental sulfur under acidic, hydrothermal conditions*. Applied and Environmental Microbiology,* **79,** 2061-2068.

Brendel PJ, Luther GWI (1995) Development of a gold amalgam voltammetric microelectrode for the determination of dissolved Fe, Mn, O2, and S (-II) in porewaters of marine and freshwater sediments*. Environmental science & technology,* **29,** 751-761.

Canavan RW, Van Cappellen P, Zwolsman JJG, van den Berg GA, Slomp CP (2007) Geochemistry of trace metals in a fresh water sediment: Field results and diagenetic modeling. *Science of The Total Environment,* **381,** 263-279.

Chislock MF, Doster E, Zitomer RA, Wilson AE (2014) Eutrophication: causes, consequences, and controls in aquatic ecosystems. *Nature Education Knowledge,* **4,**

Colmer AR, Hinkle ME (1947) The role of microorganisms in acid mine drainage: A preliminary rReport. *Science,* **106,** 253-256.

Crespo-Medina M (2009) Diversity of chemosynthetic thiosulfate oxidizing bacteria from diffuse flow hydrothermal vents and their role in mercury detoxification. Dissertation or Thesis, Rutgers University

Das SK, Mishra AK, Tindall B, Rainey FA (1996) Oxidation of thiosulfate by a new bacterium, *Bosea thiooxidans*. (strain BI-42) gen. nov., sp. nov.: Analysis of phylogeny based on chemotaxonomy and 16S ribosomal DNA sequencing. *International Journal of Systematic Bacteriology,* **46,** 981-987.

Das SK (2005) Genus V. *Bosea Das, Mishra, Tindall, Rainey and Stackebrandt 1996, 985*^{VP}. In: *Bergey's Manual® of Systematic Bacteriology* (eds Garrity G, Brenner DJ, Krieg NR, Staley JT), 2nd edn. Springer, pp 459-461.

De Giudici G, Rossi A, Fanfani L, Lattanzi P (2005) Mechanisms of galena dissolution in oxygen-saturated solutions: Evaluation of pH effect on apparent activation energies and mineral-water interface. *Geochimica et Cosmochimica Acta,* **69,** 2321-2331.

De Giudici G, Zuddas P (2001) In situ investigation of galena dissolution in oxygen saturated solution: evolution of surface features and kinetic rate. *Geochimica et Cosmochimica Acta,* **65,** 1381-1389.

De Meyer SE, Willems A (2012) Multilocus sequence analysis of *Bosea species* and description of *Bosea lupini sp*. nov., *Bosea lathyri sp*. nov. and *Bosea robiniae sp*. nov., isolated from legumes. *International Journal of Systematic and Evolutionary Microbiology,* **62,** 2505-2510.

Druschel GK, Baker BJ, Gihring TM, Banfield JF (2004) Acid mine drainage biogeochemistry at Iron Mountain, California. *Geochemical Transactions,* **5,** 13-32.

Dudka S, Adriano DC (1997) Environmental impacts of metal ore mining and processing: A review. *Journal of environmental quality,* **26,** 590.

Edelstein DL, USGS (2015) Arsenic. In: *Mineral Commodity Summaries 2015*. United States Geological Survey, pp 20-21.

Eggleton J, Thomas KV (2004) A review of factors affecting the release and bioavailability of contaminants during sediment disturbance events*. Environment international,* **30,** 973-980.

Ehrlich HL, Newman DK (2008a) Biogenesis and biodegradation of sulfide minerals at Earth's surface. In: *Geomicrobiology* (eds Ehrlich HL, Newman DK), 5th edn. CRC press, pp 491-526.

Ehrlich HL, Newman DK (2008b) Geomicrobial interactions with arsenic and antimony. In: *Geomicrobiology* (eds Ehrlich HL, Newman DK), 5th edn. CRC press, pp 491-526.

Ehrlich HL (1996) How microbes influence mineral growth and dissolution*. Chemical Geology,* **132,** 5-9.

Field D, Garrity G, Gray T, Morrison N, Selengut J, Sterk P, Tatusova T, Thomson N, Allen MJ, Angiuoli SV (2008) The minimum information about a genome sequence (MIGS) specification*. Nature biotechnology,* **26,** 541-547.

Filella M, Belzile N, Chen Y (2002) Antimony in the environment: a review focused on natural waters: I. Occurrence*. Earth-Science Reviews,* **57,** 125-176.

Filella M, Belzile N, Lett M (2007) Antimony in the environment: A review focused on natural waters. III. Microbiota relevant interactions*. Earth-Science Reviews,* **80,** 195-217.

Frau F, Medas D, Da Pelo S, Wanty R, Cidu R (2015) Environmental effects on the aquatic system and metal discharge to the Mediterranean Sea from a near-neutral zinc-ferrous sulfate mine drainage*. Water, Air, & Soil Pollution,* **226,** 1-17.

Friedrich CG, Rother D, Bardischewsky F, Quentmeier A, Fischer J (2001) Oxidation of reduced inorganic sulfur compounds by bacteria: Emergence of a common mechanism?*. Applied and Environmental Microbiology,* **67,** 2873-2882.

Gadd GM (2010) Metals, minerals and microbes: Geomicrobiology and bioremediation*. Microbiology,* **156,** 609-643.

Garrity GM, Bell JA, Lilburn T (2005a) Family VII. Bradyrhizobiaceae *fam. nov*. In: *Bergey's Manual® of Systematic Bacteriology* (eds Garrity G, Brenner DJ, Krieg NR, Staley JT). Springer, pp 438.

Garrity GM, Bell JA, Lilburn T (2005b) Class I. Alphaproteobacteria *class. nov*. In: *Bergey's Manual® of Systematic Bacteriology* (eds Garrity G, Brenner DJ, Krieg NR, Staley JT). Springer, pp 1-574.

Gene Ontology Consortium (2004) The Gene Ontology (GO) database and informatics resource*. Nucleic acids research,* **32,** D258-D261.

Ghosh W, Mallick S, DasGupta SK (2009) Origin of the Sox multienzyme complex system in ancient thermophilic bacteria and coevolution of its constituent proteins*. Research in microbiology,* **160,** 409-420.

Guberman DE, USGS (2015a) Lead. In: *Mineral Commodity Summaries 2015*, 2015th edn. United States Geological Survey, pp 90-91.

Guberman DE, USGS (2015b) Antimony. In: *Mineral Commodity Summaries 2015*, 2015th edn. United States Geological Survey, pp 18-19.

Hampton MA, Plackowski C, Nguyen AV (2011) Physical and chemical analysis of elemental sulfur formation during galena surface oxidation*. Langmuir,* **27,**4190-4201.

Hoffert JR (1947) Acid Mine Drainage*. Industrial & Engineering Chemistry,* **39,** 642-646.

Holleman A, Wiberg E (2001a) Antimony. In: *Inorganic Chemistry*, 34th edn. Academic Press, pp 757-766.

Holleman A, Wiberg E (2001b) Lead. In: *Inorganic Chemistry*, 34th edn. Academic Press, pp 912-923.

Holleman A, Wiberg E (2001c) Arsenic. In: *Inorganic Chemistry*, 34th edn. Academic Press, pp 741-757.

Hsieh YH, Huang CP (1989) The dissolution of PbS(s) in dilute aqueous solutions*. Journal of colloid and interface science,* **131,** 537-549.

Johnson DB, Hallberg KB (2005) Acid mine drainage remediation option: a review*. Science of The Total Environment,* **338,** 3-14.

Kamyshny A, Ekeltchik I, Gun J, Lev O (2006) Method for the determination of inorganic polysulfide distribution in aquatic systems*. Analytical Chemistry,* **78,** 2631-2639.

Kamyshny A, Goifman A, Gun J, Rizkov D, Lev O (2004) Equilibrium distribution of polysulfide ions in aqueous solutions at 25° C: a new approach for the study of polysulfides' equilibria. *Environmental science & technology,* **38,** 6633-6644.

Kang Y, Heinemann J, Bothner B, Rensing C, McDermott TR (2012) Integrated co-regulation of bacterial arsenic and phosphorus metabolisms. *Environmental microbiology,* **14,** 3097-3109.

Kelly DP, McDonald IR, Wood AP (2000) Proposal for the reclassification of *Thiobacillus novellus* as *Starkeya novella* gen. nov., comb. nov., in the alpha-subclass of the Proteobacteria. *International Journal of Systematic and Evolutionary Microbiology,* **50 Pt 5,** 1797-1802.

Kelly DP (1999) Thermodynamic aspects of energy conservation by chemolithotrophic sulfur bacteria in relation to the sulfur oxidation pathways. *Archives of Microbiology,* **171,**219-229.

Kelly D, Wood A (2013) The chemolithotrophic prokaryotes. In: *The Prokaryotes* (eds Rosenberg E, DeLong E, Lory S, Stackebrandt E, Thompson F). Springer Berlin Heidelberg, pp 275-287.

Kim M, Oh HS, Park SC, Chun J (2014) Towards a taxonomic coherence between average nucleotide identity and 16S rRNA gene sequence similarity for species demarcation of prokaryotes. *International Journal of Systematic and Evolutionary Microbiology,* **64,** 346-351.

Kim OS, Cho YJ, Lee K, Yoon SH, Kim M, Na H, Park SC, Jeon YS, Lee JH, Yi H, Won S, Chun J (2012) Introducing EzTaxon-e: a prokaryotic 16S rRNA gene sequence database with phylotypes that represent uncultured species. *International Journal of Systematic and Evolutionary Microbiology,* **62,** 716-721.

Konhauser KO (2009) *Introduction to geomicrobiology*. Blackwell Science Ltd, Malden, MA.

Kumar S, Stecher G, Tamura K MEGA7: Molecular Evolutionary Genetics Analysis version 7.0 for bigger datasets

Kumpiene J, Lagerkvist A, Maurice C (2008) Stabilization of As, Cr, Cu, Pb and Zn in soil using amendments – A review. *Waste Management,* **28,** 215-225.

Kuykendall LD (2005) Order Vi. Rhizobiales *ord. nov.*. In: *Bergey's Manual® of Systematic Bacteriology* (eds Garrity G, Brenner DJ, Krieg NR, Staley JT). Springer, pp 324.

La Scola B, Mallet M, Grimont PAD, Raoult D (2003) *Bosea eneae* sp. nov., *Bosea massiliensis sp*. nov. and *Bosea vestrisii sp*. nov., isolated from hospital water supplies, and emendation of the genus *Bosea* (Das et al. 1996)*. International Journal of Systematic and Evolutionary Microbiology,* **53,** 15-20.

Lehr CR, Kashyap DR, McDermott TR (2007) New insights into microbial oxidation of antimony and arsenic*. Applied and Environmental Microbiology,* **73,** 2386-2389.

Lett M, Muller D, Lièvremont D, Silver S, Santini J (2012) Unified nomenclature for genes involved in prokaryotic aerobic arsenite oxidation*. Journal of Bacteriology,* **194,** 207-208.

Li J, Wang Q, Zhang S, Qin D, Wang G (2013) Phylogenetic and genome analyses of antimony-oxidizing bacteria isolated from antimony mined soil*. International Biodeterioration & Biodegradation,* **76,** 76-80.

Luther III GW, Glazer BT, Hohmann L, Popp JI, Taillefert M, Rozan TF, Brendel PJ, Theberge SM, Nuzzio DB (2001) Sulfur speciation monitored in situ with solid state gold amalgam voltammetric microelectrodes: polysulfides as a special case in sediments, microbial mats and hydrothermal vent waters*. Journal of Environmental Monitoring,* **3,** 61-66.

Luther JM, Law M, Beard MC, Song Q, Reese MO, Ellingson RJ, Nozik AJ (2008) Schottky solar cells based on colloidal nanocrystal films*. Nano letters,* **8,** 3488-3492.

Majzlan J, Lalinská B, Chovan M, Bläß U, Brecht B, Göttlicher J, Steininger R, Hug K, Ziegler S, Gescher J (2011) A mineralogical, geochemical, and microbiological assessment of the antimony- and arsenic-rich neutral mine drainage tailings near Pezinok, Slovakia*. American Mineralogist,* **96,** 1-13.

Mandal BK, Suzuki KT (2002) Arsenic round the world: a review*. Talanta,* **58,** 201-235.

Marcondes de Souza, Jackson Antonio, Carrareto Alves LM, de Mello Varani A, de Macedo Lemos E (2014) The Family Bradyrhizobiaceae. In: *The Prokaryotes* (eds Rosenberg E, DeLong EF, Lory S, Stackebrandt E, Thompson F). Springer Berlin Heidelberg, pp 135-154.

Markowitz VM, Chen IA, Palaniappan K, Chu K, Szeto E, Grechkin Y, Ratner A, Jacob B, Huang J, Williams P, Huntemann M, Anderson I, Mavromatis K, Ivanova NN, Kyrpides NC (2012) IMG: the integrated microbial genomes database and comparative analysis system*. Nucleic acids research,* **40,** D115-D122.

Martinez CE, Jacobson AR, McBride MB (2004) Lead phosphate minerals: Solubility and dissolution by model and natural ligands. *Environmental science & technology,* **38,** 5584-5590.

Matschullat J (2000) Arsenic in the geosphere — a review. *Science of The Total Environment,* **249,** 297-312.

Meyer B, Imhoff JF, Kuever J (2007) Molecular analysis of the distribution and phylogeny of the *soxB* gene among sulfur-oxidizing bacteria - evolution of the Sox sulfur oxidation enzyme system. *Environmental microbiology,* **9,** 2957-2977.

Miretzky P, Fernandez-Cirelli A (2008) Phosphates for Pb immobilization in soils: a review. *Environmental Chemistry Letters,* **6,**121-133.

Mohapatra BR, Gould WD, Dinardo O, Koren DW (2008) An overview of the biochemical and molecular aspects of microbial oxidation of inorganic sulfur compounds. *CLEAN-- Soil, Air, Water,* **36,** 823-829.

Ng JC, Wang J, Shraim A (2003) A global health problem caused by arsenic from natural sources. *Chemosphere,* **52,** 1353-1359.

Nordstrom DK, Southam G (1997) Geomicrobiology of sulfide mineral oxidation. In: *Geomicrobiology: Interactions between Microbes and Minerals* (eds Banfield JF, Nealson KH). Reviews In Mineralogy, Washington, DC, pp 361-390.

Nordstrom DK, Blowes DW, Ptacek CJ (2015) Hydrogeochemistry and microbiology of mine drainage: An update. *Applied Geochemistry,* **57,** 3-16.

Norris PR, Clark DA, Owen JP, Waterhouse S (1996) Characteristics of *Sulfobacillus acidophilus sp*. nov. and other moderately thermophilic mineral-sulphide-oxidizing bacteria. *Microbiology,* **142,** 775-783.

Nriagu JO (1974) Lead orthophosphates—IV Formation and stability in the environment. *Geochimica et Cosmochimica Acta,* **38,** 887-898.

Okibe N, Gericke M, Hallberg KB, Johnson DB (2003) Enumeration and characterization of acidophilic microorganisms isolated from a pilot plant stirred-tank bioleaching operation. *Applied and Environmental Microbiology,* **69,** 1936-1943.

Oliva J, Cama J, Cortina JL, Ayora C, De Pablo J (2012) Biogenic hydroxyapatite (Apatite II™) dissolution kinetics and metal removal from acid mine drainage. *Journal of hazardous materials,* **213-214,** 7-18.

Ondrejkova I, Zenisova Z, Flakova R, Krcmar D, Sracek O (2013) The distribution of antimony and arsenic in waters of the Dubrava abandoned mine site, Slovak Republic. *Mine Water and the Environment,* **32,** 207-221.

Ouattara AS, Assih EA, Thierry S, Cayol J, Labat M, Monroy O, Macarie H (2003) *Bosea minatitlanensis sp*. nov., a strictly aerobic bacterium isolated from an anaerobic digester. *International Journal of Systematic and Evolutionary Microbiology,* **53,** 1247-1251.

Overbeek R, Begley T, Butler RM, Choudhuri JV, Chuang H, Cohoon M, de Crécy-Lagard V, Diaz N, Disz T, Edwards R, Fonstein M, Frank ED, Gerdes S, Glass EM, Goesmann A, Hanson A, Iwata-Reuyl D, Jensen R, Jamshidi N, Krause L, Kubal M, Larsen N, Linke B, McHardy AC, Meyer F, Neuweger H, Olsen G, Olson R, Osterman A, Portnoy V, Pusch GD, Rodionov DA, Rückert C, Steiner J, Stevens R, Thiele I, Vassieva O, Ye Y, Zagnitko O, Vonstein V (2005) The subsystems approach to genome annotation and its use in the project to annotate 1000 genomes. *Nucleic acids research,* **33,** 5691-5702.

Park JH, Bolan N (2013) Lead immobilization and bioavailability in microbial and root interface. *Journal of hazardous materials,* **261,** 777-783.

Park JH, Bolan N, Megharaj M, Naidu R (2011) Isolation of phosphate solubilizing bacteria and their potential for lead immobilization in soil. *Journal of hazardous materials,* **185,** 829-836.

Rhine ED, Ní Chadhain SM, Zylstra GJ, Young LY (2007) The arsenite oxidase genes (*aroAB*) in novel chemoautotrophic arsenite oxidizers. *Biochemical and biophysical research communications,* **354,** 662-667.

Rhine ED, Onesios KM, Serfes ME, Reinfelder JR, Young LY (2008) Arsenic transformation and mobilization from minerals by the arsenite oxidizing strain WAO. *Environmental science & technology,* **42,** 1423-1429.

Riedt CS, Buckley BT, Brolin RE, Ambia-Sobhan H, Rhoads GG, Shapses SA (2009) Blood lead levels and bone turnover with weight reduction in women. *Journal of Exposure Science and Environmental Epidemiology,* **19,** 90-96.

Robertson L, Kuenen JG (2006) The colorless sulfur bacteria. In: *The Prokaryotes* (eds Dworkin M, Falkow S, Rosenberg E, Schleifer K, Stackebrandt E), 3rd edn. Springer New York, pp 985-1011.

Rohwerder T, Sand W (2007) Mechanisms and biochemical fundamentals of bacterial metal sulfide oxidation. In: *Microbial Processing of Metal Sulfides* (eds Donati E, Sand W). Springer Netherlands, pp 35-58.

Ruby MV, Davis A, Nicholson A (1994) In situ formation of lead phosphates in soils as a method to immobilize lead. *Environmental science & technology,* **28,** 646-654.

Safronova VI, Kuznetsova IG, Sazanova AL, Kimeklis AK, Belimov AA, Andronov EE, Pinaev AG, Chizhevskaya EP, Pukhaev AR, Popov KP, Willems A, Tikhonovich IA (2015) *Bosea vaviloviae* sp. nov., a new species of slow-growing rhizobia isolated from nodules of the relict species *Vavilovia formosa* (Stev.) Fed. *Antonie van Leeuwenhoek,* **107,** 911-920.

Saini R, Kapoor R, Kumar R, Siddiqi TO, Kumar A (2011) CO_2 utilizing microbes — A comprehensive review. *Biotechnology Advances,* **29,** 949-960.

Scheckel KG, Diamond GL, Burgess MF, Klotzbach JM, Maddaloni M, Miller BW, Partridge CR, Serda SM (2013) Amending soils with phosphate as means to mitigate soil lead hazard: A critical review of the state of the science. *Journal of Toxicology and Environmental Health, Part B,* **16,** 337-380.

Shively JM, English RS, Baker SH, Cannon GC (2001) Carbon cycling: the prokaryotic contribution. *Current opinion in microbiology,* **4,** 301-306.

Shively JM, van Keulen G, Meijer WG (1998) Something from almost nothing: Carbon dioxide fixation in chemoautotrophs. *Annual Review of Microbiology,* **52,** 191-230.

Silver S, Phung LT (2005) Genes and enzymes involved in bacterial oxidation and reduction of inorganic arsenic. *Applied and Environmental Microbiology,* **71,** 599-608.

Simpson SL, Apte SC, Batley GE (1998) Effect of short-term resuspension events on trace metal speciation in polluted anoxic sediments. *Environmental science & technology,* **32,** 620-625.

Smedley PL, Kinniburgh DG (2002) A review of the source, behaviour and distribution of arsenic in natural waters. *Applied Geochemistry,* **17,** 517-568.

Stack AG, Erni R, Browning ND, Casey WH (2004) Pyromorphite growth on lead-sulfide surfaces. *Environmental Science & Technology,* **38,** 5529-5534.

Stumm W, Morgan JJ (1981) *Aquatic chemistry: an introduction emphasizing chemical equilibria in natural waters*. John Wiley

Taillefert M, Lienemann C, Gaillard J, Perret D (2000) Speciation, reactivity, and cycling of Fe and Pb in a meromictic lake. *Geochimica et Cosmochimica Acta,* **64,** 169-183.

Tamura K, Nei M (1993) Estimation of the number of nucleotide substitutions in the control region of mitochondrial DNA in humans and chimpanzees. *Molecular biology and evolution,* **10,** 512-526.

Taylor BE, Wheeler MC, Nordstrom DK (1984) Isotope composition of sulphate in acid mine drainage as measure of bacterial oxidation. *Nature,* **308,** 538-541.

Terry LR, Kulp TR, Wiatrowski H, Miller LG, Oremland RS (2015) Microbiological oxidation of antimony(III) with oxygen or nitrate by bacteria isolated from contaminated mine sediments. *Applied and Environmental Microbiology,* **81,** 8478-8488.

Torma AE, Gabra GG (1977) Oxidation of stibnite by *Thiobacillus ferrooxidans. Antonie van Leeuwenhoek,* **43,** 1-6.

Tributsch H (2001) Direct versus indirect bioleaching. *Hydrometallurgy,* **59,** 177-185.

Tsaplina I, Zhuravleva A, Belyi A, Kondrat'eva T (2010) Functional diversity of an aboriginal microbial community oxidizing the ore with high antimony content at 46–47 °C. *Microbiology,* **79,** 735-746.

U.S. EPA (2008) Lead Basic Information. *US Environmental Protection Agency,*

Wang Q, Garrity GM, Tiedje JM, Cole JR (2007) Naïve Bayesian Classifier for rapid assignment of rRNA sequences into the New Bacterial Taxonomy. *Applied and Environmental Microbiology,* **73,** 5261-5267.

Wilson C, Brigmon RL, Knox A, Seaman J, Smith G (2006) Effects of microbial and phosphate amendments on the bioavailability of lead (Pb) in shooting range soil. *Bulletin of Environmental Contamination and Toxicology,* **76,** 392-399.

Woese CR, Kandler O, Wheelis ML (1990) Towards a natural system of organisms: proposal for the domains Archaea, Bacteria, and Eucarya. *Proceedings of the National Academy of Sciences,* **87,** 4576-4579.

Xie R, Johnson W, Rodriguez L, Gounder M, Hall GS, Buckley B (2007) A study of the interactions between carboplatin and blood plasma proteins using size exclusion chromatography coupled to inductively coupled plasma mass spectrometry. *Analytical and bioanalytical chemistry,* **387,** 2815-2822.

Xie R, Johnson W, Spayd S, Hall GS, Buckley B (2007) Determination of total toxic arsenic species in human urine using hydride generation inductively coupled plasma mass spectrometry. *Journal of Analytical Atomic Spectrometry,* **22,** 553-560.

Zhang P, Ryan JA (1999) Formation of chloropyromorphite from galena (PbS) in the presence of hydroxyapatite*. Environmental science & technology,* **33,** 618-624.

Zhuravleva A, Tsaplina I, Kondrat'eva T (2011) Specific characteristics of the strains isolated from a thermoacidophilic microbial community oxidizing antimony sulfide ore*. Microbiology,* **80,** 70-81.